
**Journal of Macromolecular Science, Part A**
Publication details, including instructions for authors and subscription information:
http://www.informaworld.com/smpp/title~content=t713597274

# Heterochiral Molecular Recognition in Molecular and Macromolecular Pairs of Liquid Crystals of 4'-(11-Vinyloxyundecanyloxy)Biphenylyl (2*R*,3*S*)- and (2*S*,3*S*)-2-Fluoro-3-methylpentanoate Diastereomers

Virgil Percec[a]; Hiroji Oda[a]
[a] The W. M. Keck Laboratories for Organic Synthesis Department of Macromolecular Science Case Western Reserve University, Cleveland, Ohio

**To cite this Article** Percec, Virgil and Oda, Hiroji(1995) 'Heterochiral Molecular Recognition in Molecular and Macromolecular Pairs of Liquid Crystals of 4'-(11-Vinyloxyundecanyloxy)Biphenylyl (2*R*,3*S*)- and (2*S*,3*S*)-2-Fluoro-3-methylpentanoate Diastereomers', Journal of Macromolecular Science, Part A, 32: 8, 1531 — 1561
**To link to this Article: DOI:** 10.1080/10601329508013696
**URL:** http://dx.doi.org/10.1080/10601329508013696

J.M.S.—PURE APPL. CHEM., A32(8&9), pp. 1531–1561 (1995)

# HETEROCHIRAL MOLECULAR RECOGNITION IN MOLECULAR AND MACROMOLECULAR PAIRS OF LIQUID CRYSTALS OF 4′-(11-VINYLOXYUNDECANYLOXY)BIPHENYLYL (2*R*,3*S*)- AND (2*S*,3*S*)-2-FLUORO-3-METHYLPENTANOATE DIASTEREOMERS

VIRGIL PERCEC* and HIROJI ODA

The W. M. Keck Laboratories for Organic Synthesis
Department of Macromolecular Science
Case Western Reserve University
Cleveland, Ohio 44106-7202



## ABSTRACT

4′-(11-Vinyloxyundecanyloxy)-4-biphenylyl (2*R*,3*S*)-2-fluro-3-methylpentanoate (**15**) (2*R* 94%ee) and 4′-(11-vinyloxyundecanyloxy)-4-biphenylyl (2*S*,3*S*)-2-fluoro-3-methylpentanoate (**16**) (2*S* 90%ee) diastereomers and their corresponding homopolymers with well-defined molecular weight and narrow molecular weight distribution were synthesized and characterized. The phase behavior of **15** and poly(**15**) is quite different from those of **16** and poly(**16**), respectively. **15** displays enantiotropic $S_A$ and $S_X$ (unidentified smectic) phases and a crystalline phase, while **16** displays only a monotropic $S_A$ phase and a crystalline phase. Both poly(**15**) and poly(**16**) display enantiotropic $S_A$ and $S_{X2}$ (unidentified smectic) phases. An additional unidentified smectic phase ($S_{X1}$) was observed for both low molecular weight polymers, i.e., at DP < 5 for poly(**15**) and at DP < 9 for poly(**16**). However, the transition temperatures of poly(**15**) are 15–20°C higher than those of poly(**16**) when their phase behaviors are compared using polymers with the same molecular weight. Neither monomers nor polymers displayed an $S_C$* phase. Phase

diagrams were investigated in detail in binary mixtures of **15** with **16** and poly(**15**) with poly(**16**) as a function of the composition of the two diastereomeric structural units. In all investigated systems the diastereomeric structural units derived from the two monomers are isomorphic within all their mesophases and over the entire range of compositions. Heterochiral molecular recognition was detected only in the $S_{X1}$ phase of the polymer mixtures via a large positive deviation from the ideal values of the $S_{X1}$–$S_{X2}$ transition temperatures. On the contrary, the $S_A$–$I$ transition temperatures of all mixtures showed a good agreement with the theoretical values calculated from the Schröder–van Laar equation, suggesting that the two diastereomeric structures form an ideal solution in the $S_A$ phase and, therefore, there is no heterochiral recognition between the 2*R* and 2*S* stereogenic centers in this phase. The $S_{X1}$–$S_{X2}$ transition temperatures showed negative deviations from the ideal values, indicating the nonideal solution behavior of the two diastereomeric structural units in the $S_{X2}$ phase.



## INTRODUCTION

One of our current research interests is concerned with the heterochiral molecular recognition exhibited by molecular and macromolecular pairs of enantiomeric and diastereomeric liquid crystals. We have examined the influence of the chirality on the phase behavior of enantiomeric and diastereomeric liquid crystal mixtures in detail and observed that chiral recognition occurs specifically in layered liquid crystalline phases, and, as a consequence, it increases the phase transition temperatures of the 50/50 mixture of the two antipodes [1–3]. We also have found that the degree of chiral molecular recognition is dependent on the molecular weight in the case of macromolecular liquid crystalline pairs [2, 3].

One of the main objectives of our research is to elucidate the relationship between molecular structure and the mechanism responsible for the manifestation of the heterochiral molecular recognition, which has not yet been clarified in the limited number of papers published so far [4–7]. For this purpose we have consistently used a vinyl ether monomer containing an alkyl chain spacer and a biphenylcarboxylate mesogen, and the corresponding side chain liquid crystalline polymer obtained by the "living" cationic polymerization of the vinyl ether. "Living" cationic polymerization produces polymers with well-defined molecular weights and narrow polydispersities and, therefore, this technique is especially suitable for the synthesis of polymers used in chiral molecular recognition experiments [8, 9].

In the three papers reported so far, we used an $\alpha$-amino acid as a starting material for the synthesis of the chiral tail which was connected to the biphenylcarboxylate mesogen, and we examined the influence of steric factors (ramification, atomic size) [10–12] in the chiral tail on the chiral molecular recognition. Our current interest is focused on the influence of the connecting group between the biphenyl core and the chiral center. The first goal of this paper is to describe the synthesis and the living cationic polymerization of 4′-(11-vinyloxyundecanyloxy)-4-biphenylyl (2*R*,3*S*)-2-fluoro-3-methylpentanoate (**15**) and 4′-(11-vinyloxyundecanyloxy)-4-biphenylyl (2*S*,3*S*)-2-fluoro-3-methylpentanoate (**16**) diastereomers.

The second goal of this paper is to compare the mesomorphic behavior of these two diastereomeric structural units and to investigate the heterochiral recognition in binary monomer and polymer mixtures. The phase behavior and chiral recognition of this system will be compared to that of the system based on (2*R*,3*S*)- and (2*S*,3*S*)-2-fluoro-3-methylpentyl 4′-(11-vinyloxyundecanyloxy)biphenyl-4-carboxylate (**17**) diastereomers which was reported in detail in the first paper of this series [1].

## EXPERIMENTAL SECTION

### Materials

L-Isoleucine ((2*S*,3*S*)-(+)-2-amino-3-methylpentanoic acid, Aldrich, 99%), 2,3-dihydropyran (Lancaster, 97%), 4,4′-dihydroxybiphenyl (Aldrich, 97%), *N*,*N*′-dicyclohexyl-carbodiimide (DCC, Aldrich, 99%), *N*,*N*-dimethylaminopyridine (DMAP, Lancaster), and *n*-butyl vinyl ether (Aldrich, 98%) were used as received.

Pyridinium *p*-toluenesulfonate (PPTS) was prepared by dissolving *p*-toluenesulfonic acid in a large excess of pyridine. Crude PPTS obtained after the removal of pyridine under vacuum was recrystallized from acetone. 1,10-Phenantroline palladium(II) diacetate was prepared according to a literature procedure [9a, 13]. $CHCl_3$ was refluxed over $CaH_2$ overnight and distilled from $CaH_2$.

$CH_2Cl_2$ used as polymerization solvent was first washed with concentrated $H_2SO_4$ several times until the acid layer remained colorless, then washed with water, dried over $MgSO_4$, refluxed over $CaH_2$, and freshly distilled under argon before each use. Dimethyl sulfide [$(CH_3)_2S$] used in all polymerizations (Aldrich, anhydrous, 99+%, packed under nitrogen in Sure/Seal bottle) was used as received. Trifluoromethanesulfonic acid ($CF_3SO_3H$) used as polymerization initiator (Aldrich, 98%) was distilled under vacuum.

All other materials were commercially available and were used as received.

### Techniques

$^1$H-NMR (200 MHz) spectra were recorded on a Varian XL-200 spectrometer.

Relative molecular weights of polymers were determined by gel permeation chromatography (GPC). GPC analyses were carried out with a Perkin-Elmer Series 10LC instrument equipped with an LC-100 column oven and a Nelson Analytical 900 Series data station. Measurements were made by using a UV detector, THF as a solvent (1 mL/min, 40°C), a set of PL gel columns of $5 \times 10^2$ and $10^4$ Å, and a calibration plot constructed with polystyrene standards. High pressure liquid chromatography (HPLC) experiments were performed with the same instrument.

Two types of differential scanning calorimeters (DSC) were used to determine the thermal transition temperatures. A Perkin-Elmer DSC-4 equipped with a TADS 3600 data station was used to analyze the homopolymer poly(**15**) and the copolymers poly[**15**-*co*-[(2*R*,3*S*)-**17**]]. All other DSC analyses were performed with Perkin-Elmer PC Series DSC-7. Heating and cooling rates were 20°C/min for the analysis of the homopolymers and copolymers, and 10°C/min for the analysis of the monomer and polymer mixtures. In all cases the thermal transition temperatures were reported as the maxima and minima of their endothermic or exothermic peaks, respectively.

A Carl-Zeiss optical polarizing microscope equipped with a Mettler FP-82 hot stage and a Mettler FP-80 central processor was used to observe the thermal transitions and to analyze the anisotropic textures.

## Synthesis of Monomers

Monomers **15** and **16** were synthesized according to Scheme 1. The synthesis of compounds **2**, **3**, **4**, **5**, **7**, and **8** was described previously [1, 9].

### 1-Bromo-11-(2-tetrahydropyranyloxy)undecane (**9**)

To a solution of **8** (15.0 g, 59.7 mmol) and 2,3-dihydropyran (6.0 g, 71.7 mmol) in $CHCl_3$ (150 mL) was added a catalytic amount of PPTS (spatula tip). The mixture was stirred under gentle reflux for 2 hours. The mixture was then allowed to cool to room temperature, washed with water twice, and dried over anhydrous $MgSO_4$. The solvent was evaporated and the remaining crude product was purified by column chromatography (silica gel; hexane–ethyl acetate 20:1) to give a colorless oil (17.5 g, 87.4%), $^1$H-NMR ($CDCl_3$, TMS): $\delta$ 1.22–1.98 (m, 24H, cyclic $-OCH_2(CH_2)_3-$ and $-OCH_2(CH_2)_9CH_2Br$), 3.35–3.59 (m, 2H, $-OCH_2-(CH_2)Br$), 3.41 (t, $J$ = 6.9 Hz, 2H, $-CH_2Br$), 3.65–3.98 (m, 2H, cyclic $-OCH_2-$), 4.58 (bs, 1H, $-O(CH-)O-$).

### 4-Hydroxy-4′-[11-(2-tetrahydropyranyloxy)undecanyloxy]biphenyl (**10**)

A stirred mixture of 4,4′-dihyroxybiphenyl (9.72 g, 52.2 mmol), KOH (2.93 g, 52.2 mmol) and ethanol (80 mL) was heated to reflux. To this mixture was added dropwise a solution of **9** (17.5 g, 52.2 mmol) in ethanol (80 mL) over 30 minutes. After the whole mixture was stirred under reflux for 20 hours, 150 mL of water was added and 150 mL of ethanol was distilled off. The resulting solid was filtered, washed with water (200 mL × 2), and dried. Thin layer chromatography (TLC) analysis showed that this solid was a mixture of 4,4′-dihydroxybiphenyl, 4,4′-bis[11-(2-tetrahydropyranyloxy)undecanyloxy]biphenyl, and compound **10**. In order to remove 4,4′-dihydroxybiphenyl which was insoluble in $CH_2Cl_2$, the solid was washed with $CH_2Cl_2$ (200 mL × 2) and the solvent was evaporated from the combined filtrates to give a slightly yellow solid. Then this slightly yellow solid was washed with acetone (200 mL × 2) to separate compound **10** from 4,4′-bis[11-(2-tetrahydropyranyloxy)undecanyloxy]biphenyl which was insoluble in acetone. The solvent was evaporated from the combined filtrates to give a slightly yellow solid again. This solid was finally purified by column chromatography (silica gel; $CH_2Cl_2$–acetone 50:1) to give a white solid (9.54 g, 41.5%) which was recrystallized from ethanol (9.09 g, 39.5%). Mp 83–84°C. Purity: >99% (HPLC). $^1$H-NMR ($CDCl_3$, TMS): $\delta$ 1.21–1.96 (m, 24H, cyclic $-OCH_2(CH_2)_3-$ and $-OCH_2(CH_2)_9CH_2OPh-$), 3.34–3.59 (m, 2H, $-OCH_2(CH_2)_{10}OPh-$), 3.68–3.93 (m, 2H, cyclic $-O-CH_2-$), 3.98 (t, $J$ = 6.6 Hz, 2H, $-CH_2OPh-$), 4.62 (bs, 1H, $-O(CH-)O-$), 5.62 (s, 1H, $-PhOH$), 6.89 (d, $J$ = 8.5 Hz, 2ArH, ortho to $-OH$), 6.95 (d, $J$ = 8.7 Hz, 2ArH, ortho to $-(CH_2)_{11}O-$), 7.43 (d, $J$ = 8.5 Hz, 2ArH, meta to $-OH$), 7.46 (d, $J$ = 8.7 Hz, 2ArH, meta to $-(CH_2)_{11}O-$).

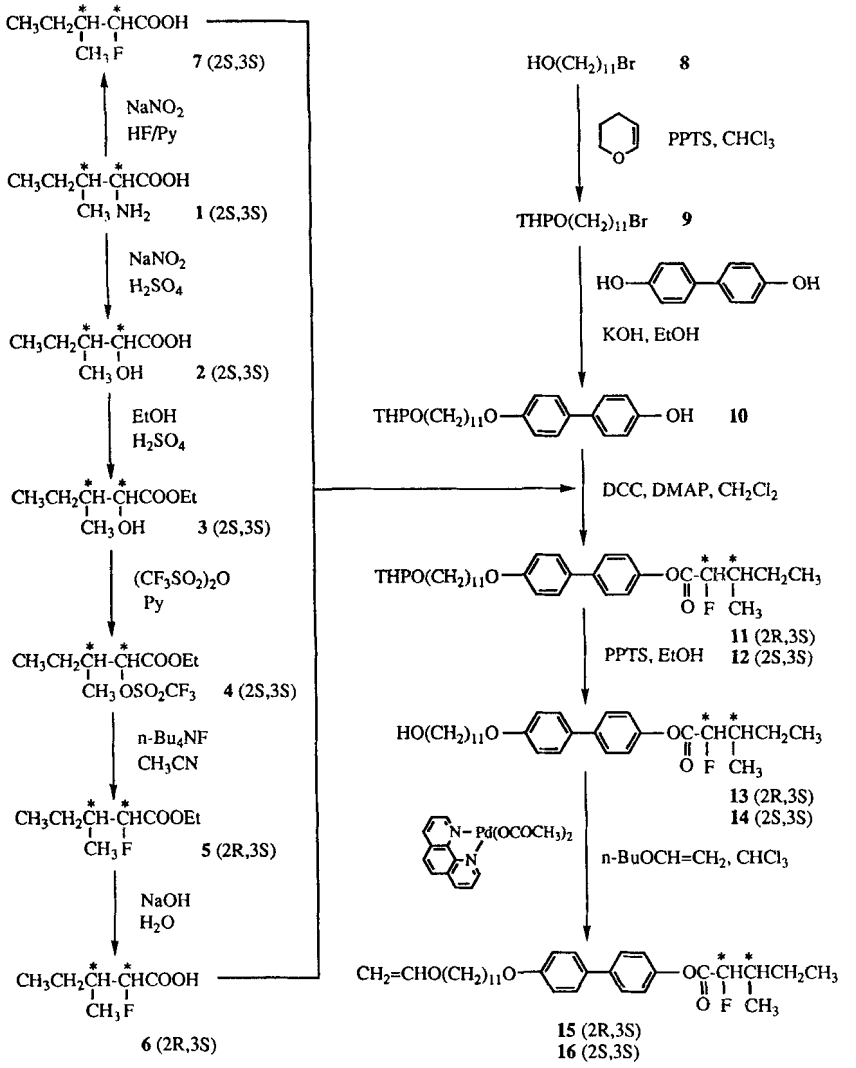


SCHEME 1. Synthesis of monomers **15** and **16**.

## (2*R*,3*S*)-2-Fluoro-3-methylpentanoic Acid (**6**)

A mixture of **5** (5.65 g, 34.9 mmol), NaOH (6.0 g, 150 mmol), and water (100 mL) was stirred at room temperature for 16 hours. The solution was acidified by concentrated HCl and the product was extracted into diethyl ether three times. The combined ethereal extracts were dried over anhydrous $MgSO_4$. The solvent was evaporated and the remaining crude product was distilled under vacuum to give a colorless oil (4.10 g, 87.5%). Bp 79–82°C (5 mmHg). $^1$H-NMR ($CDCl_3$, TMS): $\delta$ 0.99 (t, $J$ = 6.8 Hz, 3H, $-CH_2C\underline{H}_3$), 1.00 (d, $J$ = 6.1 Hz, 3H, $-CH(C\underline{H}_3)-$), 1.28–1.70 (m, 2H, $-C\underline{H}_2CH_3$), 1.83–2.20 (m, 1H, $-CH(C\underline{H}_3)-$), 4.95 (dd, $J$ = 49.0 and 2.7 Hz, 1H, $-C\underline{H}F-$), 11.35 (bs, 1H, $-COO\underline{H}$).

### 4′-[11-(2-Tetrahydropyranyloxy)undecanyloxy]-4-biphenylyl (2*R*,3*S*)-2-Fluoro-3-methylpentanoate (11)

To a stirred mixture of **10** (7.93 g, 18.0 mmol), DCC (3.71 g, 18.0 mmol), DMAP (0.66 g, 5.4 mmol), and dry $CH_2Cl_2$ (80 mL) was added a solution of **6** (2.42 g, 18.0 mmol) in dry $CH_2Cl_2$ (20 mL) at room temperature. Stirring was continued at room temperature for 3 hours and the resulting white precipitate was filtered off. The filtrate was washed with water twice and dried over anhydrous $MgSO_4$. The solvent was evaporated and the remaining crude product was purified by column chromatography (silica gel; hexane–ethyl acetate 30:1 and 20:1) to give a white solid (8.57 g, 85.5%). Mp 68–70°C. Purity: >99% (HPLC). $^1$H-NMR ($CDCl_3$, TMS): $\delta$ 1.04 (t, $J$ = 7.4 Hz, 3H, $-CH_2C\underline{H}_3$), 1.10 (d, $J$ = 7.1 Hz, 3H, $-CH(C\underline{H}_3)-$), 1.23–1.96 (m, 26H, cyclic $-OCH_2(C\underline{H}_2)_3-$, $-OCH_2(C\underline{H}_2)_9CH_2OPh-$, and $-C\underline{H}_2CH_3$), 1.96–2.35 (m, 1H, $-C\underline{H}(CH_3)-$), 3.32–3.57 (m, 2H, $-OC\underline{H}_2(CH_2)_{10}OPh-$), 3.67–3.95 (m, 2H, cyclic $-OC\underline{H}_2-$), 3.99 (t, $J$ = 6.6 Hz, 2H, $-C\underline{H}_2OPh-$), 4.58 (bs, 1H, $-O(C\underline{H}-)O-$), 5.13 (dd, $J$ = 49.0 and 3.0 Hz, 1H, $-C\underline{H}F-$), 6.97 (d, $J$ = 8.7 Hz, 2ArH, ortho to $-(CH_2)_{11}O-$), 7.16 (d, $J$ = 8.5 Hz, 2ArH, ortho to $-OCO-$), 7.49 (d, $J$ = 8.7 Hz, 2ArH, meta to $-(CH_2)_{11}O-$), 7.57 (d, $J$ = 8.5 Hz, 2ArH, meta to $-OCO-$).

### 4′-(11-Hydroxyundecanyloxy)-4-biphenylyl (2*R*,3*S*)-2-Fluro-3-methylpentanoate (13)

A catalytic amount of PPTS (spatula tip) was added to a solution of **11** (8.57 g, 15.4 mmol) in ethanol (150 mL) and the mixture was stirred at 80°C for 2 hours. Ethanol was evaporated and the remaining solid was dissolved in ether, washed with water, and dried over anhydrous $MgSO_4$. The solvent was evaporated and the remaining crude product was purified by column chromatography (silica gel; $CH_2Cl_2$–acetone 100:1 and 40:1) to give a white solid (6.61 g, 90.8%) which was recrystallized from ethanol (6.13 g, 84.2%). Mp 106–107°C. Purity: >99% (HPLC). $^1$H-NMR ($CDCl_3$, TMS): $\delta$ 1.04 (t, $J$ = 7.4 Hz, 3H, $-CH_2C\underline{H}_3$), 1.10 (d, $J$ = 7.1 Hz, 3H, $-CH(C\underline{H}_3)-$), 1.25–1.90 (m, 20H, $HOCH_2(C\underline{H}_2)_9CH_2O-$ and $-C\underline{H}_2CH_3$), 1.95–2.32 (m, 1H, $-C\underline{H}(CH_3)-$), 3.65 (t, $J$ = 6.5 Hz, 2H, $HOC\underline{H}_2-$), 4.00 (t, $J$ = 6.5 Hz, 2H, $HO(CH_2)_{10}C\underline{H}_2OPh-$), 5.13 (dd, $J$ = 48.8 and 3.0 Hz, 1H, $-C\underline{H}F-$), 6.97 (d, $J$ = 8.7 Hz, 2ArH, ortho to $HO(CH_2)_{11}O-$), 7.17 (d, $J$ = 8.7 Hz, 2ArH, ortho to $-OCO-$), 7.49 (d, $J$ = 8.7 Hz, 2ArH, meta to $HO(CH_2)_{11}O-$), 7.57 (d, $J$ = 8.7 Hz, 2ArH, meta to $-OCO-$).

### 4′-(11-Vinyloxyundecanyloxy)-4-biphenylyl (2*R*,3*S*)-2-Fluro-3-methylpentanoate (15)

A mixture of **13** (2.5 g, 5.3 mmol), 1,10-phenanthroline palladium(II) diacetate (0.202 g, 0.50 mmol), *n*-butyl vinyl ether (26.5 mL) and dry $CHCl_3$ (7.0 mL) was stirred at 60°C for 16 hours under a nitrogen atmosphere. The dark green precipitate was filtered off and excess *n*-butyl vinyl ether and $CHCl_3$ were evaporated. The remaining crude product was purified twice by column chromatography (silica gel; hexane–ethyl acetate 20:1) to give a white solid (1.54 g, 58.3%). Purity: >99% (HPLC). The transition temperatures are given in Table 4. $^1$H-NMR ($CDCl_3$, TMS): $\delta$ 1.04 (t, $J$ = 7.5 Hz, 3H, $-CH_2C\underline{H}_3$), 1.10 (d, $J$ = 7.1 Hz,

3H, $-CH(C\underline{H}_3)-$), 1.26-1.88 (m, 20H, $-OCH_2(C\underline{H}_2)_9CH_2O-$ and $-C\underline{H}_2CH_3$), 1.99-2.31 (m, 1H, $-C\underline{H}(CH_3)-$), 3.68 (t, $J$ = 6.6 Hz, 2H, $CH_2=CHOC\underline{H}_2-$), 4.00 (t, $J$ = 6.6 Hz, 2H, $-(CH_2)_{10}C\underline{H}_2OPh-$ and dd, $J$ = 6.7, 1.7 Hz, 1H, $C\underline{H}_2$ =CH−trans), 4.17 (dd, $J$ = 14.4 and 1.7 Hz, 1H, $C\underline{H}_2$=CH− cis), 5.13 (dd, $J$ = 49.0 and 3.0 Hz, 1H, $-C\underline{H}F-$), 6.48 (dd, $J$ = 14.4 and 6.7 Hz, 1H, $CH_2=C\underline{H}-$), 6.97 (d, $J$ = 8.7 Hz, 2ArH, ortho to $-O(CH_2)_{11}O-$), 7.17 (d, $J$ = 8.5 Hz, 2ArH, ortho to −OCO−), 7.49 (d, $J$ = 8.7 Hz, 2ArH, meta to $-O(CH_2)_{11}O-$), 7.56 (d, $J$ = 8.5 Hz, 2ArH, meta to −OCO−).

### 4′-[11-(2-Tetrahydropyranyloxy)undecanyloxyl-4-biphenylyl (2*S*,3*S*)-2-Fluro-3-methylpentanoate (**12**)

**12** was synthesized by the same procedure as the one used for the preparation of **11**. Starting from 8.50 g (19.3 mmol) of **10**, 2.59 g (19.3 mmol) of **7**, 3.98 g (19.3 mmol) of DCC, 0.71 g (5.8 mmol) of DMAP, and 100 mL of dry $CH_2Cl_2$, 9.28 g (86.4%) of **12** was obtained as a white solid. Mp 56-58°C. Purity: >99% (TLC). $^1$H-NMR ($CDCl_3$, TMS): $\delta$ 1.02 (t, $J$ = 7.5 Hz, 3H, $-CH_2C\underline{H}_3$), 1.15 (d, $J$ = 6.9 Hz, 3H, $-CH(C\underline{H}_3)-$), 1.22-2.04 (m, 26H, cyclic $-OCH_2(C\underline{H}_2)_3-$, $-OCH_2(C\underline{H}_2)_9CH_2OPh-$ and $-C\underline{H}_2CH_3$), 2.04-2.36 (m, 1H, $-C\underline{H}(CH_3)-$), 3.28-3.59 (m, 2H, $-OC\underline{H}_2(CH_2)_{10}OPh-$), 3.68-3.94 (m, 2H, cyclic $-OC\underline{H}_2-$), 4.00 (t, $J$ = 6.4 Hz, 2H, $-C\underline{H}_2OPh-$), 4.58 (bs, 1H, $-O(C\underline{H}-)O-$), 5.02 (dd, $J$ = 48.7 and 4.6 Hz, 1H, $-C\underline{H}F-$), 6.97 (d, $J$ = 8.8 Hz, 2ArH, ortho to $-(CH_2)_{11}O-$), 7.17 (d, $J$ = 8.5 Hz, 2ArH, ortho to −OCO−), 7.49 (d, $J$ = 8.8 Hz, 2ArH, meta to $-(CH_2)_{11}O-$), 7.57 (d, $J$ = 8.5 Hz, 2ArH, meta to −OCO−).

### 4′-(11-Hydroxyundecanyloxy)-4-biphenylyl (2*S*,3*S*)-2-Fluoro-3-methylpentanoate (**14**)

**14** was synthesized by the same procedure as the one used for the preparation of **13**. Starting from 8.75 g (15.7 mmol) of **12**, a catalytic amount of PPTS (spatula tip) and 150 mL of ethanol, 6.59 g (88.8%) of **14** was obtained as a white solid. Mp 97-98°C. Purity: >99% (TLC). $^1$H-NMR ($CDCl_3$, TMS): $\delta$ 1.02 (t, $J$ = 7.4 Hz, 3H, $-CH_2C\underline{H}_3$), 1.15 (d, $J$ = 6.8 Hz, 3H, $-CH(C\underline{H}_3)-$), 1.22-1.90 (m, 20H, $HOCH_2(C\underline{H}_2)_9CH_2O-$ and $-C\underline{H}_2CH_3$), 2.02-2.34 (m, 1H, $-C\underline{H}(CH_3)-$), 3.65 (t, $J$ = 6.5 Hz, 2H, $HOC\underline{H}_2-$), 4.00 (t, $J$ = 6.5 Hz, 2H, $HO(CH_2)_{10}-C\underline{H}_2OPh-$), 5.02 (dd, $J$ = 48.6 and 4.4 Hz, 1H, $-C\underline{H}F-$), 6.97 (d, $J$ = 8.7 Hz, 2ArH, ortho to $HO(CH_2)_{11}O-$), 7.17 (d, $J$ = 8.7 Hz, 2ArH, ortho to −OCO−), 7.49 (d, $J$ = 8.7 Hz, 2ArH, meta to $HO(CH_2)_{11}O-$), 7.57 (d, $J$ = 8.7 Hz, 2ArH, meta to −OCO−).

### 4′-(11-Vinyloxyundecanyloxy)-4-biphenylyl (2*S*,3*S*)-2-Fluoro-3-methylpentanoate (**16**)

**16** was synthesized by the same procedure as the one used for the preparation of **15**. Starting from 3.00 g (6.30 mmol) of **14**, 0.243 g (0.600 mmol) of 1,10-phenanthroline palladium(II) diacetate, 31.5 mL of *n*-butyl vinyl ether and 8.5 mL of dry $CHCl_3$, 1.40 g (44.6%) of **16** was obtained as a white solid. Purity: >99% (TLC). The transition temperatures are given in Table 4. $^1$H-NMR ($CDCl_3$, TMS): $\delta$ 1.01 (t, $J$ = 7.4 Hz, 3H, $-CH_2C\underline{H}_3$), 1.15 (d, $J$ = 6.9 Hz, 3H, $-CH(C\underline{H}_3)-$),

1.23–1.86 (m, 20H, $-OCH_2(C\underline{H}_2)_9CH_2O-$ and $-C\underline{H}_2CH_3$), 2.04–2.33 (m, 1H, $-C\underline{H}(CH_3)-$), 3.67 (t, $J$ = 6.5 Hz, 2H, $CH_2=CHOC\underline{H}_2-$), 3.99 (t, $J$ = 6.3 Hz, 2H, $-(CH_2)_{10}C\underline{H}_2OPh-$ and dd, $J$ = 6.8 and 1.8 Hz, 1H, $C\underline{H}_2=CH-$ trans), 4.17 (dd, $J$ = 14.4 and 1.8 Hz, 1H, $C\underline{H}_2=CH-$ cis), 5.01 (dd, $J$ = 48.6 and 4.4 Hz, 1H, $-C\underline{H}F-$), 6.48 (dd, $J$ = 14.4 and 6.8 Hz, 1H, $CH_2=C\underline{H}-$), 6.97 (d, $J$ = 8.7 Hz, 2ArH, ortho to $-O(CH_2)_{11}O-$), 7.16 (d, $J$ = 8.7 Hz, 2ArH, ortho to $-OCO-$), 7.49 (d, $J$ = 8.7 Hz, 2ArH, meta to $-O(CH_2)_{11}O-$), 7.56 (d, $J$ = 8.7 Hz, 2ArH, meta to $-OCO-$).

### Cationic Polymerization

Polymerizations were carried out in a three-neck round bottom flask equipped with a Teflon stopcock and rubber septa under an argon atmosphere at 0°C for 1 hour. All glassware was dried overnight at 140°C. The monomer was further dried under vacuum overnight in the polymerization flask. After the flask was filled with argon, freshly distilled dry $CH_2Cl_2$ was added via a syringe and the solution was cooled to 0°C. $(CH_3)_2S$ and $CF_3SO_3H$ were then added carefully via a syringe. The monomer concentration was about 0.224 M and the $(CH_3)_2S$ concentration was 10 times larger than that of $CF_3SO_3H$. The polymer molecular weight was controlled by the monomer/initiator ($[M]_0/[I]_0$) ratio. After quenching the polymerization with methanol, the reaction mixture was poured into a large amount of methanol to give a white precipitate. The obtained polymer was purified by reprecipitation by pouring its chloroform solution into methanol, and dried under vacuum.



## RESULTS AND DISCUSSION

### Determination of the Optical Purities of Monomers 15 and 16

The synthesis of the two diastereomeric monomers **15** and **16** is outlined in Scheme 1. The transformations of the starting material, L-isoleucine **1**, into compounds **5** and **7** were described in a previous publication [1]. The amino group of L-isoleucine was first converted into hydroxy (compound **2**) and fluorine (compound **7**) groups, respectively, via a diazonium salt. These substitution reactions proceed with the retention of configuration at the C2 position due to the anchimeric assistance of the carboxylate group. Compound **2** was further converted into triflate **4**, which was substituted with a fluorine atom by using *n*-$Bu_4NF$ followed by the hydrolysis of the ethyl ester to afford compound **6**. Since the substitution of the triflate with the fluorine atom proceeds with Walden inversion of configuration at the C2 position, compound **6** is expected to have (2*R*,3*S*) configurations, while compound **7** has (2*S*,3*S*) configurations. Compounds **6** and **7** are expected to be transformed into monomers **15** and **16** without any change of their configurations during the other steps of the synthesis.

Figure 1 presents the 200 MHz $^1$H-NMR spectra of monomers **15** and **16**. It is clear that the proton signals associated with the C2 chiral center (k proton) have different chemical shifts between monomers **15** (Fig. 1a, 5.13 ppm) and **16** (Fig. 1b, 5.01 ppm). The optical purities calculated from the integrals of these peaks are 2*R* 97% (94%ee) for monomer **15** and 2*S* 95% (90%ee) for monomer **16**. The optical

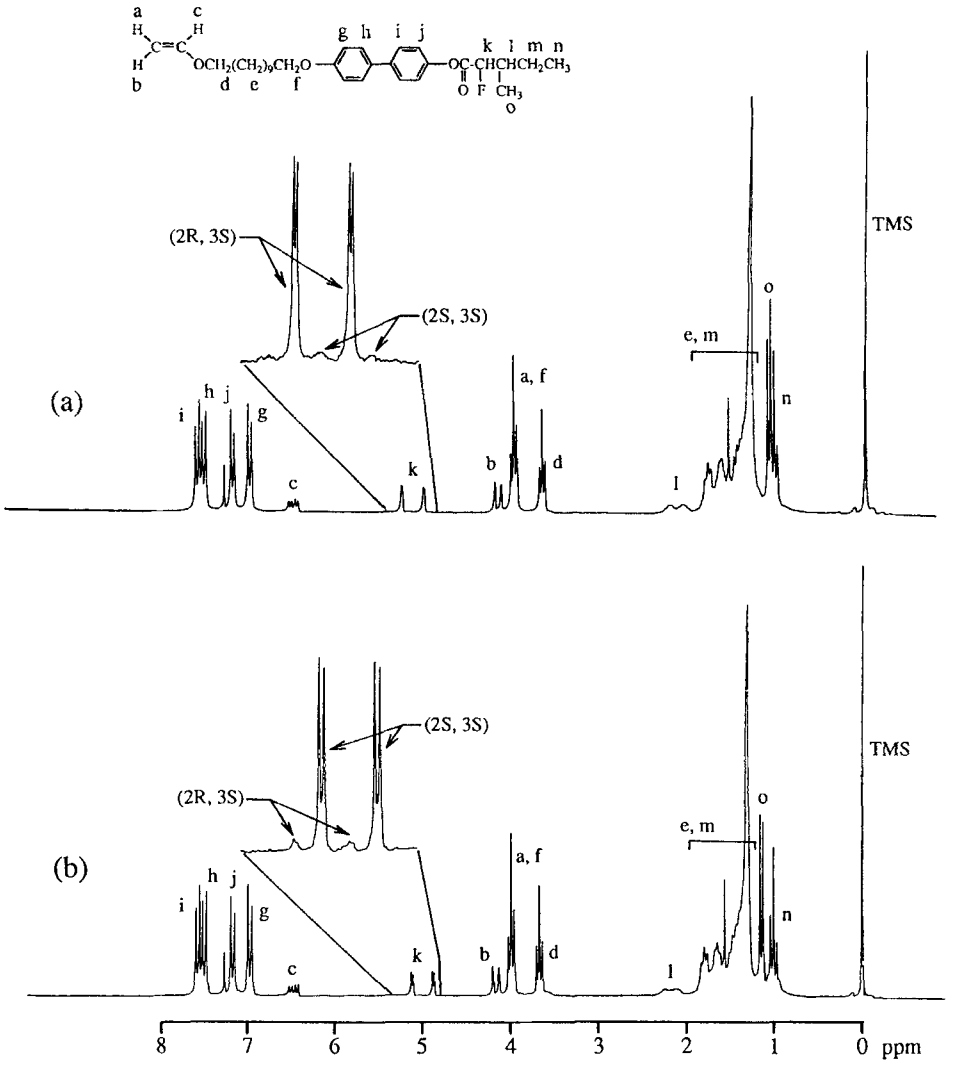


FIG. 1. $^1$H-NMR spectra of monomers **15** (a) and **16** (b).

purity arising from the C3 chiral center was not able to be determined because proton 1 of monomer **15** showed an almost identical chemical shift to that of monomer **16**. However, it is believed that the original optical purity of L-isoleucine is maintained at the C3 chiral center because of its chemical stability, and this is supported by the different chemical shifts of the methyl protons (o protons) on the C3 chiral center in Fig. 1.

From our previous experience the chiral centers of the monomers are insensitive to the cationic polymerization conditions, and the original optical purities of monomers remain unchanged during the polymerization process [1–3].

## Homopolymerization of 15 and 16

The homopolymerizations of **15** and **16** are presented in Scheme 2. All polymerizations were carried out at 0°C in $CH_2Cl_2$ by a "living" cationic polymerization technique using $CF_3SO_3H/(CH_3)_2S$ as initiating system. Previous work in our laboratory [14] and others [15] has shown that the $CF_3SO_3H$-initiated polymerization of vinyl ethers in the presence of a Lewis base such as $(CH_3)_2S$ gives well-defined polymers with controlled molecular weights and narrow polydispersities. The polymerization mechanism is discussed in detail in previous publications [8, 9, 14].

The characterization of poly(**15**) and poly(**16**) by gel permeation chromatography (GPC) and differential scanning calorimetry (DSC) is summarized in Tables 1 and 2, respectively. The low polymer yields are the result of the loss of polymer during purification. Relative number-average molecular weights of polymers determined by GPC exhibit a linear dependence on the initial molar ratio of monomer to initiator ($[M]_0/[I]_0$) as shown in Fig. 2. All polydispersities are lower than 1.20. The $[M]_0/[I]_0$ ratio provides a very good control of the polymer molecular weight. All these features demonstrate the typical characteristics of a living polymerization mechanism.

The mesomorphic behavior of poly(**15**) and poly(**16**) was investigated by DSC and thermal optical polarized microscopy. Figures 3 and 4 present the DSC thermograms of poly(**15**) and poly(**16**) with various degrees of polymerization (DP), respectively. The dependence of phase transition temperatures on DP was plotted in Fig. 5(a-c) [poly(**15**)] and 5(d-f) [poly(**16**)]. As observed from these figures, poly(**15**) and poly(**16**) exhibit similar phase behaviors. However, the transition temperatures of poly(**15**) are 15-20°C higher than those of poly(**16**) when their phase transitions are compared using polymers with the same molecular weight. On the first heating scan, all polymers show a crystalline melting peak followed by two smectic phases. On the second and subsequent heating scans, another endothermic peak is observed instead of the crystalline melting peak. This endothermic peak seems to be a transition peak between two higher order smectic phases ($S_{X1}$ and $S_{X2}$) in lower molecular weight polymers, i.e., at DP < 5 for poly(**15**) and at DP < 9

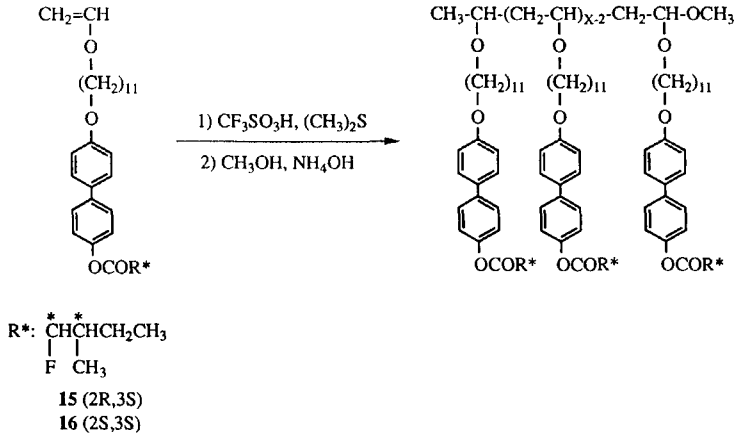


SCHEME 2. Cationic polymerization of monomers **15** and **16**.

TABLE 1. Cationic Polymerization of 4′-(11-Vinyloxyundecanyloxy)-4-biphenylyl (2*R*,3*S*)-2-Fluoro-3-methylpentanoate (**15**) and Characterization of the Resulting Polymers[a]

| Sample | $[M]_0/[I]_0$ | Polymer yield, % | GPC | | | Phase transitions (°C) and corresponding enthalpy changes (kcal/mru)[b] | |
|---|---|---|---|---|---|---|---|
| | | | $M_n \times 10^{-3}$ | $M_W/M_n$ | DP | Heating | Cooling |
| 1 | 2 | 39.7 | 1.73 | 1.04 | 3.5 | *K* 65.9 (4.21) $S_{X2}$ 90.9 (1.13) $S_A$ 105.2 (1.70) *I*<br>$S_{X1}$ 66.4 (2.11) $S_{X2}$ 89.9 (1.19) $S_A$ 104.6 (1.77) *I* | *I* 99.5 (−1.73) $S_A$ 84.4 (−1.09) $S_{X2}$ 51.2 (−2.01) $S_{X1}$ |
| 2 | 3 | 62.7 | 2.18 | 1.08 | 4.4 | *K* 63.5 (2.75) $S_{X2}$ 96.2 (1.11) $S_A$ 116.0 (1.82) *I*<br>$S_{X1}$ 70.7 (1.41) $S_{X2}$ 96.0 (1.18) $S_A$ 116.4 (1.82) *I* | *I* 110.1 (−1.75) $S_A$ 89.6 (−1.15) $S_{X2}$ 59.3 (−1.26) $S_{X1}$ |
| 3 | 5 | 55.8 | 2.59 | 1.10 | 4.7 | *K* 74.1 (2.10) $S_{X2}$ 99.1 (1.21) $S_A$ 122.8 (1.77) *I*<br>$S_{X1}$ 79.6 (1.05) $S_{X2}$ 98.5 (1.19) $S_A$ 122.8 (1.75) *I* | *I* 115.2 (−1.75) $S_A$ 91.7 (−1.18) $S_{X2}$ 67.5 (−0.81) $S_{X1}$ |
| 4 | 8 | 65.5 | 3.70 | 1.14 | 7.4 | *K* 75.1 (0.98) $S_{X2}$ 116.9 (2.14) $S_A$ 139.7 (1.61) *I*<br>*g* 96.2 $S_{X2}$ 114.7 (2.31) $S_A$ 136.8 (1.63) *I* | *I* 128.6 (−1.68) $S_A$ 101.6 (−2.10) $S_{X2}$ 86.9 *g* |
| 5 | 16 | 73.4 | 4.31 | 1.11 | 8.5 | *K* 79.2 (1.98) $S_{X2}$ 121.5 (2.20) $S_A$ 146.1 (1.65) *I*<br>*g* 102.6 $S_{X2}$ 121.7 (2.36) $S_A$ 145.8 (1.56) *I* | *I* 139.2 (−1.62) $S_A$ 109.5 (−2.22) $S_{X2}$ 95.3 *g* |
| 6 | 20 | 70.4 | 5.73 | 1.13 | 11.5 | *K* 83.3 (1.66) $S_{X2}$ 129.4 (2.24) $S_A$ (1.55) *I*<br>*g* 110.8 $S_{X2}$ 129.1 (2.50) $S_A$ 153.2 (1.48) *I* | *I* 146.5 (−1.52) $S_A$ 116.7 (−2.35) $S_{X2}$ 103.6 *g* |
| 7 | 30 | 76.0 | 7.40 | 1.12 | 14.8 | *K* 83.3 (1.33) $S_{X2}$ 133.8 (2.38) $S_A$ 157.9 (1.45) *I*<br>*g* 113.6 $S_{X2}$ 133.1 (2.61) $S_A$ 157.6 (1.43) *I* | *I* 150.8 (−1.43) $S_A$ 120.5 (−2.44) $S_{X2}$ 105.7 *g* |

[a]Polymerization temperature, 0°C; polymerization solvent, $CH_2Cl_2$; $[M]_0 = 0.224$; $[Me_2S]_0/[I]_0 = 10$; polymerization time, 1 hour.

[b]Data on the first line are from first heating and cooling scans. Data on the second line are from second heating scan. Heating and cooling rates are 20°C/min.

TABLE 2. Cationic Polymerization of 4′-(11-Vinyloxyundecanyloxy)-4-biphenylyl (2*R*,3*S*)-2-Fluoro-3-methylpentanoate (**16**) and Characterization of the Resulting Polymers[a]

| Sample | $[M]_0/[I]_0$ | Polymer yield, % | GPC | | | Phase transitions (°C) and corresponding enthalpy changes (kcal/mru)[b] | |
|---|---|---|---|---|---|---|---|
| | | | $M_n \times 10^{-3}$ | $M_W/M_n$ | DP | Heating | Cooling |
| 1 | 2 | 18.6 | 1.88 | 1.08 | 3.8 | *K* 50.9 (3.81) $S_{X2}$ 73.0 (1.37) $S_A$ 95.5 (1.60) *I*<br>$S_{X1}$ 67.0 (1.83) $S_{X2}$ 72.4 (1.22) $S_A$ 95.2 (1.57) *I* | *I* 87.3 (−1.55) $S_A$ 65.0 (−1.42) $S_{X2}$ 55.8 (−1.75) $S_{X1}$ |
| 2 | 8 | 75.6 | 3.69 | 1.18 | 7.4 | *K* 56.7 (0.95) $S_{X2}$ 100.1 (1.80) $S_A$ 120.5 (1.44) *I*<br>$S_{X1}$ 80.1 (1.14) $S_{X2}$ 99.4 (1.67) $S_A$ 120.5 (1.44) *I* | *I* 111.7 (−1.49) $S_A$ 86.4 (−1.94) $S_{X2}$ 72.7 (−0.87) $S_{X1}$ |
| 3 | 12 | 71.6 | 4.48 | 1.20 | 9.0 | *K* 55.8 (1.70) $S_{X2}$ 106.3 (2.06) $S_A$ 125.6 (1.34) *I*<br>$S_{X1}$ 79.9 (0.69) $S_{X2}$ 105.7 (1.91) $S_A$ 126.3 (1.36) *I* | *I* 117.1 (−1.35) $S_A$ 90.6 (−1.71) $S_{X2}$ 67.6 (−0.28) $S_{X1}$ |
| 4 | 16 | 68.9 | 5.68 | 1.13 | 11.4 | *K* 57.7 (1.60) $S_{X2}$ 111.0 (1.97) $S_A$ 133.9 (1.38) *I*<br>*g* 84.0 $S_{X2}$ 110.7 (1.94) $S_A$ 133.4 (1.36) *I* | *I* 125.0 (−1.37) $S_A$ 96.8 (−1.94) $S_{X2}$ 74.6 *g* |
| 5 | 25 | 80.5 | 7.24 | 1.13 | 14.5 | *K* 58.9 (1.09) $S_{X2}$ 118.5 (2.33) $S_A$ 140.0 (1.25) *I*<br>*g* 84.9 $S_{X2}$ 118.3 (2.38) $S_A$ 139.7 (1.24) *I* | *I* 131.8 (−1.27) $S_A$ 105.0 (−2.32) $S_{X2}$ 74.6 *g* |

[a]Polymerization temperature, 0°C; polymerization solvent, $CH_2Cl_2$; $[M]_0 = 0.224$; $[Me_2S]_0/[I]_0 = 10$; polymerization time, 1 hour.

[b]Data on the first line are from first heating and cooling scans. Data on the second line are from second heating scan. Heating and cooling rates are 20°C/min.

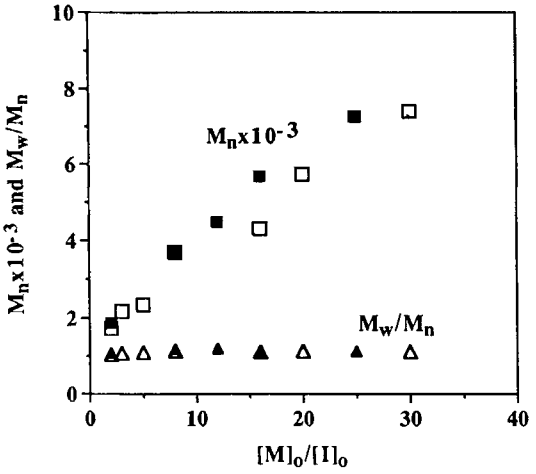


FIG. 2. Dependence of the number-average molecular weight ($M_n$) and polydispersity ($M_w/M_n$) of poly(**15**) (open symbols) and poly(**16**) (closed symbols) determined by GPC on the $[M]_0/[I]_0$ ratio.



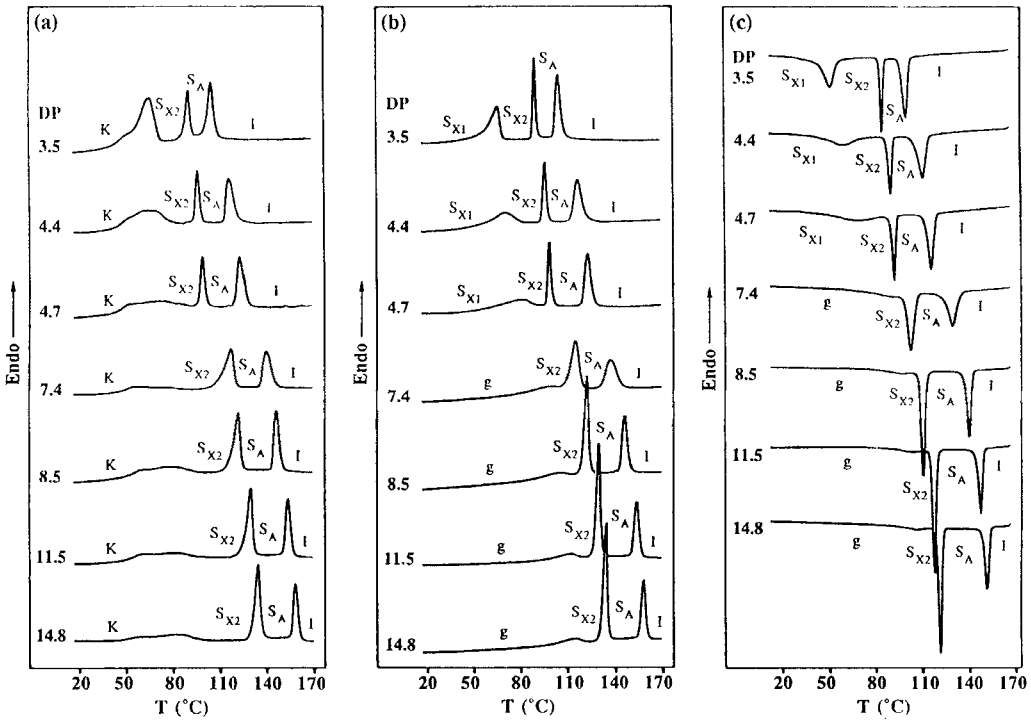


FIG. 3. DSC thermograms (20°C/min) of poly(**15**) with different degrees of polymerization (DP): (a) first heating scans; (b) second heating scans; (c) first cooling scans.

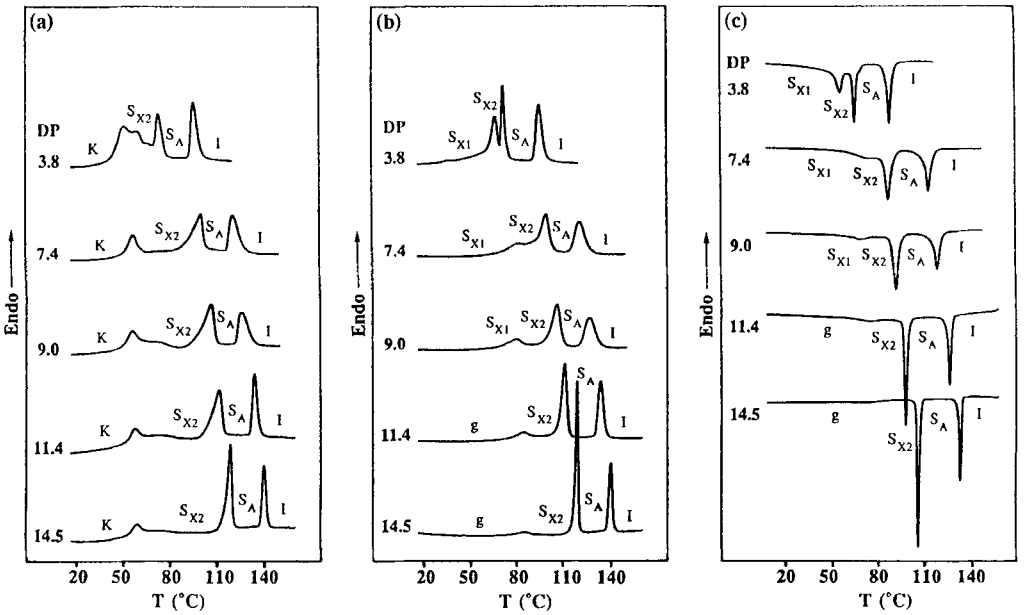


FIG. 4. DSC thermograms (20°C/min) of poly(**16**) with different DP: (a) first heating scans; (b) second heating scans; (c) first cooling scans.



for poly(**16**). In higher molecular weight polymers, on the other hand, it seems that this peak represents a glass transition. The three smectic phases observed in the second heating scan are enantiotropic and reproducible on the subsequent heating and cooling scans. Polarized optical microscope analysis showed that the highest temperature smectic phase of both diastereomeric homopolymers was a smectic A phase, whereas the nature of the two lower temperature (higher order) smectic phases was not yet identified. Representative optical polarized micrographs of the texture exhibited by the $S_A$ and $S_{X2}$ phases of poly(**15**) (DP = 8.5) and poly(**16**) (DP = 14.5) are presented in Fig. 6.

In order to confirm the above phase assignment, copolymerization experiments between monomer **15** and (2*R*,3*S*)-2-fluoro-3-methylpentyl 4′-(vinyloxyundecanyloxy)biphenyl-4-carboxylate [(**2*R*,3*S*)-17**], whose homopolymer displays $S_A$ and $S_C^*$ phases [1], were performed. Based on our previous experience, copolymers derived from two monomers which lead to two homopolymers displaying the same mesophase will show a continuous dependence of their phase transitions on copolymer composition. On the contrary, if the structural units of these two homopolymers are not isomorphic within a particular mesophase, a triple point will occur on the phase diagram [9b, 9d, 16]. Scheme 3 illustrates the copolymerization of **15** with (**2*R*,3*S*)-17**. Attempts were made to synthesize poly[(**15**)-*co*-[(**2*R*,3*S*)-17**]]X/Y (where X/Y refers to the mole ratio of the two structural units) with DP = 20. The copolymerization results are summarized in Table 3. The copolymer yields are lower than quantitative due to the polymer loss during the purification process.

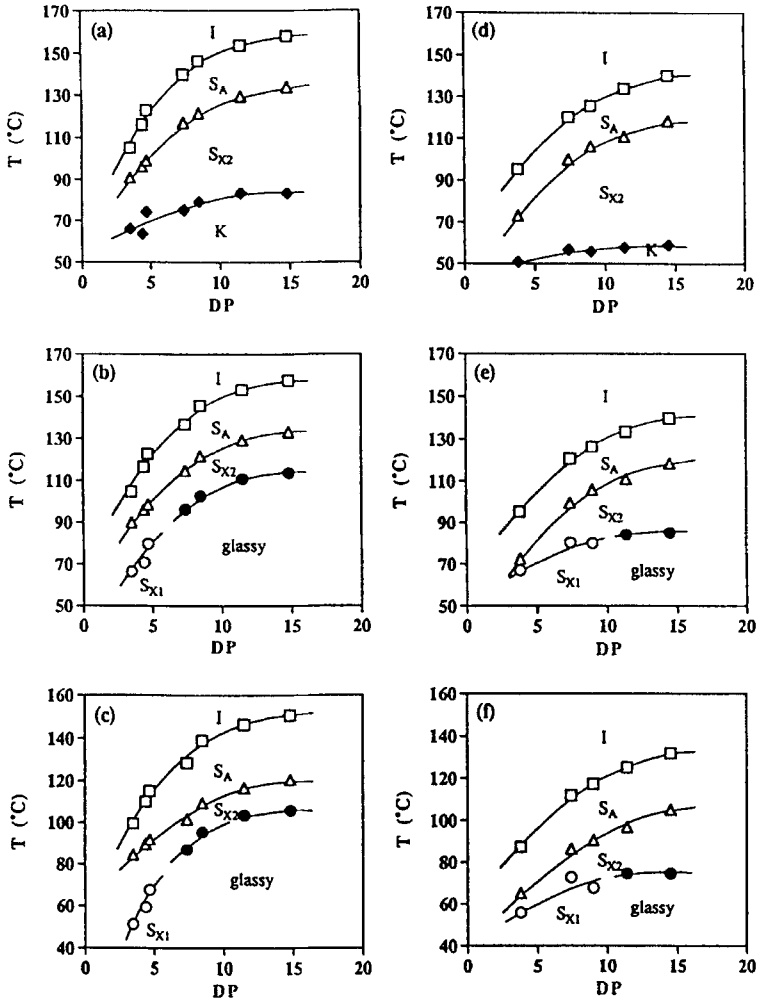


FIG. 5. Dependence of phase transition temperatures on the DP of poly(**15**) (a-c) and poly(**16**) (d-f): (a, d) data from the first heating scans; (b, e) data from the second heating scans; (c, f) data from the first cooling scans.

However, all conversions were quantitative and, therefore, the copolymer composition is identical to that of the monomer feed [8]. The DSC traces and the phase diagrams of the copolymers are presented in Figs. 7 and 8, respectively. It is clear from these figures that the $S_A$ and the higher order smectic ($S_{X2}$) phases display a continuous dependence over the entire composition range, while the $S_C$* phase of poly[(**2*R*,3*S*)-17**] disappears at X/Y = 50/50 with a triple point. These results support the above phase assignment of poly(**15**) and also confirm the fact that poly(**15**) does not exhibit a $S_C$* mesophase.

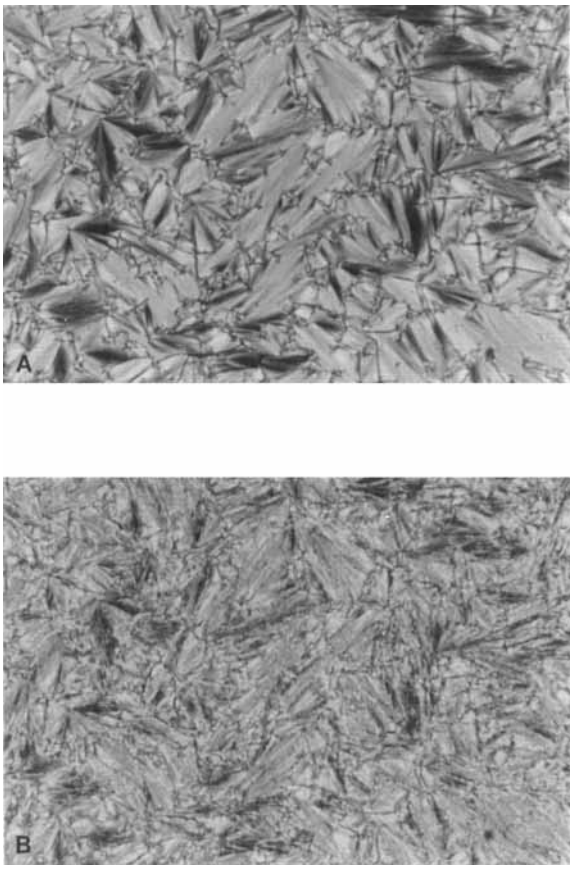


FIG. 6. Representative optical polarized micrographs of: (A) the $S_A$ mesophase displayed by poly(**15**) (DP = 8.5) upon cooling to 130°C; (B) the $S_{X2}$ mesophase displayed by poly(**15**) (DP = 8.5) upon cooling to 108°C; (C) the $S_A$ mesophase displayed by poly(**16**) (DP = 14.5) upon cooling to 130°C; (D) the $S_{X2}$ mesophase displayed by poly(**16**) (DP = 14.5) upon cooling to 103°C.

The structural difference between **15** and (**2*R*,3*S*)-17** lies in the direction of the ester function which connects the biphenyl core and the chiral tail. The copolymerization experiments of monomer **15** with (**2*R*,3*S*)-17** are clearly demonstrating that the reversal of the ester linkage of (**2*R*,3*S*)-17** gives way to the disappearance of the $S_C$* phase in poly(**15**). This result is consistent with the previous findings by Goodby et al. (for low molar mass liquid crystals) [17] and by Vairon et al. (for side chain liquid crystalline polymers) [18]. As described by Goodby and Leslie [17], the reversal of the ester function disrupts the conjugation of the carbonyl group with the delocalized electrons of the biphenyl core in the biphenylcarboxylate mesogen of poly[(**2*R*,3*S*)-17**] and the resulting less polarized nature of biphenyl mesogen in poly(**15**) is responsible for the disappearance of the tilted $S_C$* phase.

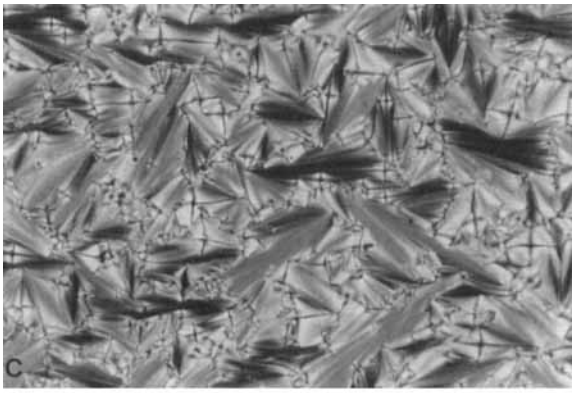


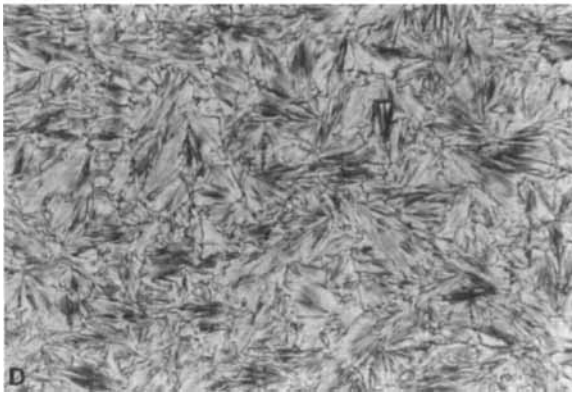




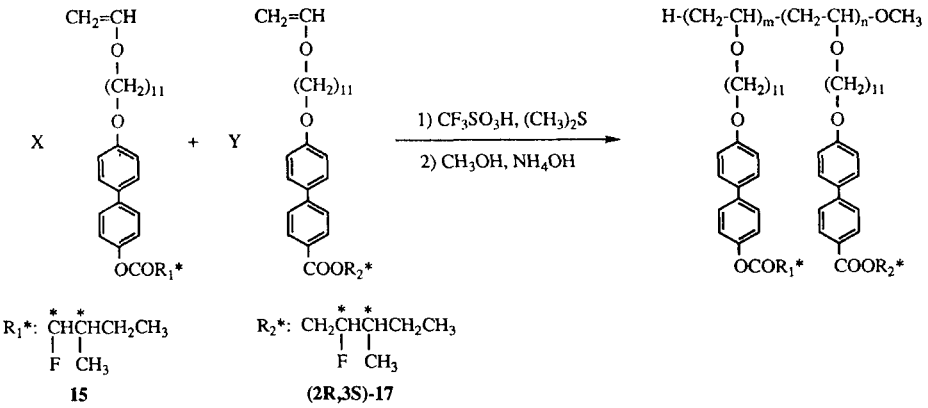


**15** **(2R,3S)-17**

SCHEME 3. Cationic copolymerization of **15** (a) and **16** (b).

TABLE 3. Cationic Copolymerization of (**15**) with (**2*R*,3*S*)-*17*** and Characterization of the Resulting Polymers[a]

| [**15**]/[(**2*R*, 3*S*)-17**], mol/mol | Polymer yield, % | GPC | | | Phase transitions (°C) and corresponding enthalpy changes (kcal/mru)[b] | |
|---|---|---|---|---|---|---|
| | | $M_n \times 10^{-3}$ | $M_w/M_n$ | DP | Heating | Cooling |
| 0/100 | 85.8 | 6.10 | 1.20 | 11.8 | *K* 59.0 (†[c]) $S_{X2}$ 61.4 (1.83) $S_C$* 94.2 (0.03) $S_A$ 124.3 (1.40) *I*<br>$S_{X2}$ 62.9 (1.22) $S_C$* 95.7 (0.07) $S_A$ 126.1 (1.43) *I* | *I* 119.4 (−1.40) $S_A$ 91.3 (−0.06) $S_C$* 57.5 (−1.12) $S_{X2}$ |
| 10/90 | 73.3 | 6.85 | 1.08 | 13.4 | *K* 58.9 (0.66) $S_{X2}$ 63.9 (0.94) $S_C$* 92.7 (0.05) $S_A$ 126.2 (1.43) *I*<br>$S_{X2}$ 64.0 (0.93) $S_C$* 92.4 (0.03) $S_A$ 126.2 (1.41) *I* | *I* 119.7 (−1.41) $S_A$ 88.0 (−0.04) $S_C$* 58.1 (−0.88) $S_{X2}$ |
| 20/80 | 63.7 | 6.57 | 1.07 | 12.9 | *K* 59.7 (0.61) $S_{X2}$ 67.2 (0.99) $S_C$* 91.4 (0.02) $S_A$ 128.2 (1.45) *I*<br>$S_{X2}$ 68.8 (0.92) $S_C$* 91.3 (0.04) $S_A$ 128.4 (1.42) *I* | *I* 121.2 (−1.42) $S_A$ 86.0 (−0.05) $S_C$* 62.0 (−0.92) $S_{X2}$ |
| 30/70 | 69.4 | 4.91 | 1.14 | 9.7 | *K* 55.9 (1.11) $S_{X2}$ 66.2 (0.80) $S_C$* 86.6 (0.03) $S_A$ 122.0 (1.57) *I*<br>$S_{X2}$ 65.6 (0.85) $S_C$* 86.0 (0.03) $S_A$ 121.8 (1.54) *I* | *I* 115.3 (−1.54) $S_A$ 81.6 (−0.04) $S_C$* 60.0 (−0.86) $S_{X2}$ |
| 40/60 | 67.6 | 5.28 | 1.17 | 10.4 | *K* 56.6 (0.94) $S_{X2}$ 74.8 (0.91) $S_C$* 86.1 (0.09) $S_A$ 126.1 (1.57) *I*<br>$S_{X2}$ 74.6 (0.98) $S_C$* 85.5 (0.08) $S_A$ 125.8 (1.56) *I* | *I* 120.0 (−1.57) $S_A$ 81.5 (−0.08) $S_C$* 68.3 (−1.03) $S_{X2}$ |
| 50/50 | 67.2 | 6.22 | 1.09 | 12.3 | *K* 68.1 (1.42) $S_{X2}$ 87.0 (1.30) $S_A$ 137.6 (1.45) *I*<br>$S_{X2}$ 87.6 (1.44) $S_A$ 137.6 (1.44) *I* | *I* 129.4 (−1.43) $S_A$ 82.2 (−0.06) $S_C$* 78.2 (−1.25) $S_{X2}$ |
| 60/40 | 54.8 | 6.70 | 1.07 | 13.3 | *K* 72.7 (1.53) $S_{X2}$ 96.0 (1.64) $S_A$ 140.3 (1.62) *I*<br>$S_{X2}$ 96.0 (1.62) $S_A$ 140.2 (1.42) *I* | *I* 133.8 (−1.72) $S_A$ 87.3 (−1.80) $S_{X2}$ |
| 70/30 | 75.7 | 4.80 | 1.11 | 9.5 | *K* 70.6 (1.20) $S_{X2}$ 99.3 (1.35) $S_A$ 139.5 (1.58) *I*<br>*g* 74.5 $S_{X2}$ 99.4 (1.63) $S_A$ 139.7 (1.55) *I* | *I* 131.6 (−1.55) $S_A$ 88.5 (−1.57) $S_{X2}$ |
| 80/20 | 78.8 | 5.92 | 1.18 | 11.8 | *K* 56.5 (0.92) $S_{X2}$ 107.6 (1.60) $S_A$ 142.1 (1.55) *I*<br>*g* 82.5 $S_{X2}$ 107.0 (1.50) $S_A$ 141.6 (1.51) *I* | *I* 135.7 (−1.54) $S_A$ 96.1 (−1.54) $S_{X2}$ |
| 90/10 | 76.5 | 5.86 | 1.21 | 11.7 | *K* 58.2 (1.00) $S_{X2}$ 118.4 (1.88) $S_A$ 146.0 (1.53) *I*<br>*g* 94.4 $S_{X2}$ 117.5 (2.08) $S_A$ 146.3 (1.50) *I* | *I* 140.1 (−1.56) $S_A$ 105.1 (−1.85) $S_{X2}$ 86.8 *g* |
| 100/0 | 70.4 | 5.73 | 1.13 | 11.5 | *K* 83.3 (1.66) $S_{X2}$ 129.4 (2.24) $S_A$ 153.4 (1.55) *I*<br>*g* 110.8 $S_{X2}$ 129.1 (2.50) $S_A$ 153.2 (1.48) *I* | *I* 146.5 (−1.52) $S_A$ 116.7 (−2.35) $S_{X2}$ 103.6 (−0.15) $S_{X1}$ |

[a]Polymerization temperature, 0°C; polymerization solvent, $CH_2Cl_2$; $[M]_0$ = [**15**]/[(**2*R*,3*S*)-17**] = 0.224; $[M]_0/[I]_0$ = 20; $[Me_2S]_0/[I]_0$ = 10; polymerization time, 1 hour.

[b]Data on the first line are from first heating and cooling scans. Data on the second line are from second heating scan. Heating and cooling rates are 20°C/min.

[c]Overlapped peak.

## Miscibility Studies

Monomers **15** and **16** were mixed in various compositions and the phase behavior of their mixtures was investigated by DSC. Mixtures were prepared by dissolving the two monomers in $CH_2Cl_2$ followed by evaporation of the solvent under vacuum. Three sets of binary mixtures between poly(**15**) and poly(**16**) with different molecular weights were also prepared and their phase behaviors were investigated in the same manner. The molecular weights and polydispersities of the polymers employed in this miscibility study are as follows: polymer mixture I: poly(**15**) with DP = 4.7, $M_w/M_n$ = 1.10 and poly(**16**) with DP = 9.0, $M_w/M_n$ = 1.20; polymer mixture II: poly(**15**) with DP = 8.5, $M_w/M_n$ = 1.11 and poly(**16**) with DP = 12.5, $M_w/M_n$ = 1.14; polymer mixture III: poly(**15**) with DP = 14.8, $M_w/M_n$ = 1.12 and poly(**16**) with DP = 14.5, $M_w/M_n$ = 1.13. The thermal transition temperatures and the corresponding enthalpy changes are summarized in Table 4 for the monomer mixtures and Tables 5–7 for the polymer mixtures. The phase diagrams of the monomer mixtures are presented in Fig. 9 and the phase diagrams of the polymer mixtures are presented in Figs. 10–12. The DSC thermograms of the monomer mixtures and polymer mixture I are presented in Figs. 13 and 14, respectively.

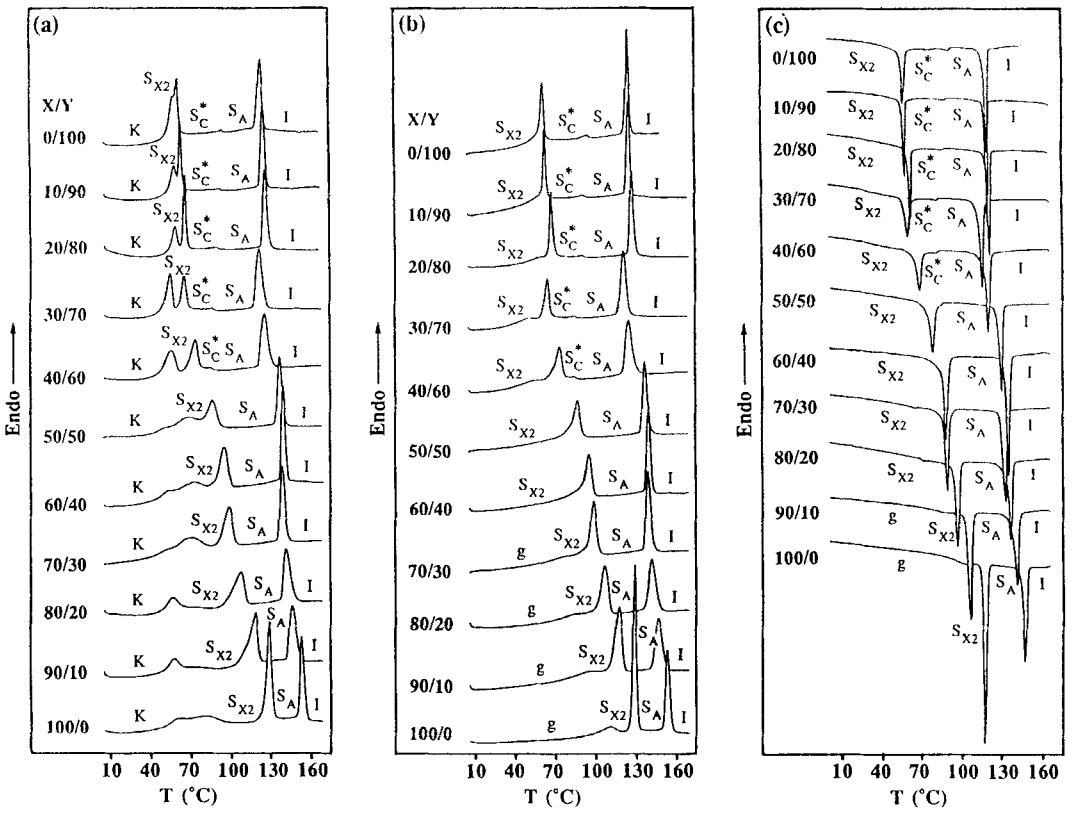


FIG. 7. DSC thermograms (20°C/min) of poly[**15**-*co*-[(2*R*,3*S*)-**17**]]X/Y with different compositions: (a) first heating scans; (b) second heating scans; (c) first cooling scans.

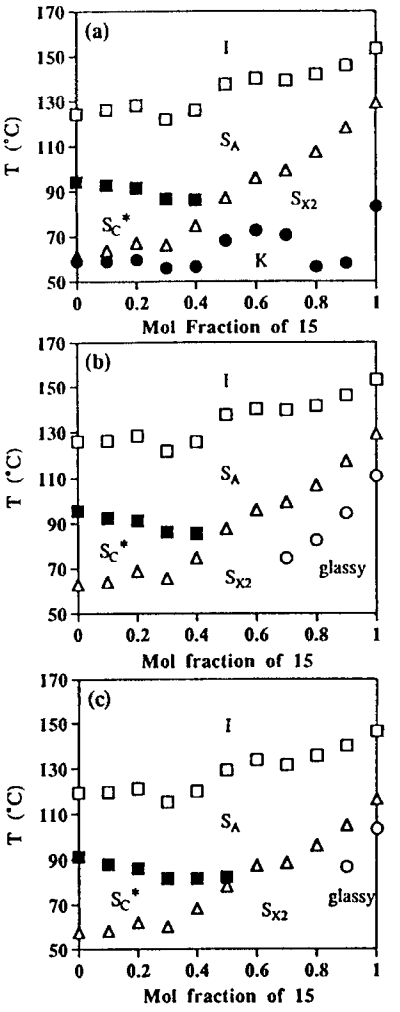


FIG. 8. Dependence of phase transition temperatures on the composition of poly[**15**-*co*-[(2*R*,3*S*)-**17**]].

The phase behavior of monomer **15** is different from that of monomer **16**. As the corresponding polymer poly(**15**) showed 15–20°C higher transition temperatures than poly(**16**) with the same molecular weight, the isotropization temperature of monomer **15** is *ca.* 14°C higher than that of monomer **16**. However, crystalline melting and crystallization temperatures for both monomers are almost identical and, as a consequence, monomer **15** exhibits enantiotropic $S_A$ and $S_X$ (unidentified smectic) phases, while monomer **16** exhibits only a monotropic $S_A$ mesophase.

When the two monomers are mixed, their $S_A$ phases showed a continuous dependence on the mixture composition and are found to be isomorphic. The $S_A$–$I$ transition temperatures display a slight upward curvature, i.e., a positive deviation

TABLE 4. Characterization of the Binary Mixtures of Monomers **15** and **16**

| **15/16**, (mol)/(mol) | Phase transitions (°C) and corresponding enthalpy changes (kcal/mol)[a] | |
|---|---|---|
| | Heating | Cooling |
| 0/100 | *K* 44.8 (3.48) *K* 46.0 (−1.11) *K* 51.0 (7.71) *I*<br>*K*50.8 (7.58) *I* | *I* 48.8 (−1.24) $S_A$ 37.1 (−6.13) *K* |
| 10.7/89.3 | *K* 42.0 (2.14) *K* 43.9 (−0.56) *K* 50.5 (5.92) $S_A$ 54.1 (1.18) *I*<br>*K* 50.3 (6.27) $S_A$ 54.1 (1.33) *I* | *I* 50.6 (−1.28) $S_A$ 34.6 (−5.97) *K* |
| 20.6/79.4 | *K* 40.5 (2.05) *K* 42.1 (−0.30) *K* 50.5 (6.25) $S_A$ 55.8 (1.33) *I*<br>*K* 50.4 (6.31) $S_A$ 55.8 (1.39) *I* | *I* 52.1 (−1.34) $S_A$ 35.6 (†[b]) $S_X$ 33.3 (−5.93) *K* |
| 30.7/69.3 | *K* 38.9 (1.90) *K* 40.5 (−0.06) *K* 50.6 (6.08) $S_A$ 57.3 (1.38) *I*<br>*K* 50.4 (6.08) $S_A$ 57.3 (1.34) *I* | *I* 53.7 (−1.34) $S_A$ 37.8 (−0.97) $S_X$ 32.4 (−4.84) *K* |
| 40.7/59.3 | *K* 36.9 (1.89) *K* 38.8 (−0.21) *K* 50.5 (60.3) $S_A$ 58.7 (1.38) *I*<br>*K* 50.3 (6.14) $S_A$ 58.7 (1.38) *I* | *I* 55.3 (−1.41) $S_A$ 40.1 (−0.91) $S_X$ 31.8 (−4.91) *K* |
| 50.6/49.4 | *K* 37.3 (1.74) *K* 38.5 (−0.18) *K* 50.9 (6.17) $S_A$ 60.3 (1.44) *I*<br>*K* 49.1 (†[b]) *K* 50.8 (6.25) $S_A$ 60.2 (1.43) *I* | *I* 56.6 (−1.46) $S_A$ 42.3 (−0.95) $S_X$ 31.4 (−5.00) *K* |
| 59.5/40.5 | *K* 37.6 (2.02) *K* 50.2 (7.09) $S_A$ 61.5 (1.66) *I*<br>*K* 50.0 (7.14) $S_A$ 61.5 (1.65) *I* | *I* 57.9 (−1.66) $S_A$ 44.2 (−1.10) $S_X$ 31.6 (−5.76) *K* |
| 69.4/30.6 | *K* 38.0 (2.13) *K* 51.0 (7.96) $S_A$ 63.1 (1.92) *I*<br>*K* 51.0 (7.96) $S_A$ 63.0 (1.89) *I* | *I* 59.1 (−1.88) $S_A$ 46.4 (−1.29) $S_X$ 31.6 (−6.54) *K* |
| 80.0/20.0 | *K* 37.8 (1.54) *K* 39.1 (−0.27) *K* 50.9 (7.87) $S_A$ 64.2 (1.92) *I*<br>*K* 51.3 (7.96) $S_A$ 64.2 (1.89) *I* | *I* 60.6 (−1.91) $S_A$ 48.9 (−1.36) $S_X$ 32.5 (−6.62) *K* |
| 90.0/10.0 | *K* 38.8 (1.50) *K* 39.7 (−0.60) *K* 51.1 (†[b]) *K* 54.1 (6.04) $S_A$ 65.6 (1.56) *I*<br>*K* 52.2 (6.28) $S_X$ 54.9 (†[b]) $S_A$ 65.6 (1.54) *I* | *I* 61.8 (−1.51) $S_A$ 51.1 (−1.08) $S_X$ 33.6 (−5.04) *K* |
| 100/0 | *K* 54.9 (6.60) $S_X$ 57.2 (†[b] $S_A$ 66.7 (1.53) *I*<br>*K* 53.2 (4.92) $S_X$ 57.0 (1.08) $S_A$ 66.6 (1.53) *I* | *I* 63.0 (−1.52) $S_A$ 53.3 (−1.08) $S_X$ 34.8 (−4.84) *K* |

[a]Data on the first line are from first heating and cooling scans. Data on the second line are from second heating scan. Heating and cooling rates are 10°C/min.

[b]Overlapped peak.

TABLE 5. Characterization of the Binary Mixtures of Poly(**15**) (DP = 4.7, $M_w/M_n$ = 1.10) with Poly(**16**) (DP = 9.0, $M_w/M_n$ = 1.20) (polymer mixture I)

| Poly(**15**)/ poly(**16**), (mol/mol) | Phase transitions (°C) and corresponding enthalpy changes (kcal/mru)[a] | |
|---|---|---|
| | Heating | Cooling |
| 0/100 | *K* 51.5 (2.67) $S_{X2}$ 103.9 (2.33) $S_A$ 122.7 (1.45) *I*<br>*g* 72.0 $S_{X1}$ 78.6 (0.32) $S_{X2}$ 104.2 (1.63) $S_A$ 123.9 (1.40) *I* | *I* 119.5 (−1.46) $S_A$ 93.3 (−1.75) $S_{X2}$ 72.3 (−0.45) $S_{X1}$ 69.3 *g* |
| 10.0/90.0 | *K* 61.2 (1.95) $S_{X2}$ 102.0 (2.35) $S_A$ 122.8 (1.41) *I*<br>*g* $S_{X1}$ 75.7 (0.39)[b] $S_{X2}$ 101.9 (1.54) $S_A$ 122.9 (1.51) *I* | *I* 118.8 (−1.51) $S_A$ 91.6 (−1.60) $S_{X2}$ 71.8 (−0.19) $S_{X1}$ *g*[b] |
| 20.3/79.7 | *K* 63.2 (0.38) $S_{X2}$ 99.9 (1.83) $S_A$ 121.4 (1.33) *I*<br>*g* 73.0 $S_{X1}$ 78.9 (0.08) $S_{X2}$ 99.3 (1.25) $S_A$ 122.2 (1.34) *I* | *I* 117.8 (−1.49) $S_A$ 89.6 (−1.43) $S_{X2}$ 75.4 (−0.06) $S_{X1}$ 64.5 *g* |
| 39.9/60.1 | *K* 56.8 (1.37) $S_{X2}$ 93.4 (1.82) $S_A$ 120.0 (1.54) *I*<br>*g* 73.3 $S_{X1}$ 83.0 (†[b]) $S_{X2}$ 94.2 (1.58) $S_A$ 120.3 (1.49) *I* | *I* 116.4 (−1.60) $S_A$ 86.8 (−1.77) $S_{X2}$ 79.4 (†[b]) $S_{X1}$ 63.3 *g* |
| 49.9/50.1 | *K* 56.8 (0.97) $S_{X2}$ 91.4 (1.66) $S_A$ 119.0 (1.49) *I*<br>*g* 73.4 $S_{X1}$ 84.9 (†[b]) $S_{X2}$ 92.5 (1.54) $S_A$ 120.0 (1.45) *I* | *I* 115.6 (−1.58) $S_A$ 85.8 (−1.66) $S_{X2}$ 81.9 (†[b]) $S_{X1}$ 61.0 *g* |
| 60.0/40.0 | *K* 59.6 (1.29) $S_{X2}$ 89.7 (1.67) $S_A$ 118.4 (1.56) *I*<br>*g* 71.2 $S_{X1}$ 87.8 (†[b]) $S_{X2}$ 89.5 (1.48) $S_A$ 118.9 (1.53) *I* | *I* 114.9 (−1.67) $S_A$ 85.3 (−1.60) $S_{X1}$ 60.4 *g* |
| 79.8/20.2 | *K* 58.4 (2.00) $S_{X2}$ 90.6 (1.47) $S_A$ 117.4 (1.59) *I*<br>*g* 71.3 $S_{X1}$ 84.5 (†[b]) $S_{X2}$ 90.5 (1.16) $S_A$ 117.7 (1.60) *I* | *I* 113.4 (−1.69) $S_A$ 86.2 (−1.21) $S_{X2}$ 80.9 (†[b]) $S_{X1}$ 61.5 *g* |
| 89.8/10.2 | *K* 59.8 (2.08) $S_{X2}$ 91.8 (1.18) $S_A$ 117.1 (1.68) *I*<br>*g* 72.1 $S_{X1}$ 80.0 (†[b]) $S_{X2}$ 91.2 (1.18) $S_A$ 117.1 (1.69) *I* | *I* 112.6 (−1.73) $S_A$ 86.9 (−1.17) $S_{X2}$ 77.5 (−0.07) $S_{X1}$ 63.0 *g* |
| 100/0 | *K* 51.9 (1.99) $S_{X2}$ 92.6 (1.21) $S_A$ 116.2 (1.72) *I*<br>*g* 71.0 $S_{X1}$ 75.8 (†[b]) $S_{X2}$ 92.3 (1.20) $S_A$ 116.8 (1.78) *I* | *I* 112.4 (−1.77) $S_A$ 88.2 (−1.18) $S_{X2}$ 64.3 *g* |

[a]Data on the first line are from first heating and cooling scans. Data on the second line are from second heating scan. Heating and cooling rates are 10°C/min.

[b]Overlapped peak.

TABLE 6. Characterization of the Binary Mixtures of Poly(**15**) (DP = 8.5, $M_w/M_n$ = 1.11) with Poly(**16**) (DP = 12.5, $M_w/M_n$ = 1.14) (polymer mixture II)

| Poly(**15**)/ poly(**16**), (mol)/(mol) | Phase transitions (°C) and corresponding enthalpy changes (kcal/mru)[a] | |
|---|---|---|
| | Heating | Cooling |
| 0/100 | *K* 54.9 (1.41) $S_{X2}$ 114.6 (2.26) $S_A$ 135.8 (1.24) *I*<br>*g* 82.6 $S_{X2}$ 114.7 (2.25) $S_A$ 135.8 (1.23) *I* | *I* 131.2 (−1.24) $S_A$ 104.8 (−2.18) $S_{X2}$ 75.7 *g* |
| 10.0/90.0 | *K* 59.8 (0.98) $S_{X2}$ 114.0 (2.24) $S_A$ 136.0 (1.23) *I*<br>*g* 78.8 $S_{X2}$ 113.9 (2.13) $S_A$ 136.2 | *I* 131.7 (−1.28) $S_A$ 104.5 (−2.11) $S_{X2}$ 69.9 *g* |
| 19.1/80.9 | *K* 60.7 (2.04 $S_{X2}$ 113.6 (2.18) $S_A$ 136.6 (1.28) *I*<br>*g* 77.7 $S_{X2}$ 113.5 (2.15) $S_A$ 136.8 (1.30) *I* | *I* 132.2 (−1.31) $S_A$ 104.3 (−2.10) $S_{X2}$ 70.2 *g* |
| 39.8/60.2 | *K* 60.7 (1.71) $S_{X2}$ 113.2 (2.08) $S_A$ 138.0 (1.31) *I*<br>*g* 78.1 $S_{X2}$ 112.9 (2.08) $S_A$ 138.1 (1.31) *I* | *I* 133.5 (−1.37) $S_A$ 104.4 (−2.04) $S_{X2}$ 69.3 *g* |
| 50.1/49.9 | *K* 59.6 (0.99) $S_{X2}$ 113.1 (2.06) $S_A$ 138.8 (1.31) *I*<br>*g* 80.2 $S_{X2}$ 113.3 (2.03) $S_A$ 139.0 (1.32) *I* | *I* 134.2 (−1.35) $S_A$ 104.7 (−1.96) $S_{X2}$ 73.5 *g* |
| 59.1/40.9 | *K* 63.4 (1.71) $S_{X2}$ 113.3 (2.06) $S_A$ 139.0 (1.31) *I*<br>*g* 80.5 $S_{X2}$ 113.4 (1.99) $S_A$ 139.1 (1.34) *I* | *I* 134.5 (−1.38) $S_A$ 104.9 (−1.98) $S_{X2}$ 74.7 *g* |
| 79.7/20.3 | *K* 63.2 (2.55) $S_{X2}$ 114.8 (1.99) $S_A$ 140.8 (1.40) *I*<br>*g* 88.0 $S_{X2}$ 114.8 (2.02) $S_A$ 140.4 (1.42) *I* | *I* 135.4 (−1.49) $S_A$ 105.3 (−1.97) $S_{X2}$ 82.5 *g* |
| 89.9/10.1 | *K* 64.6 (2.61) $S_{X2}$ 116.4 (2.14) $S_A$ 141.1 (1.48) *I*<br>*g* 93.3 $S_{X2}$ 115.8 (2.13) $S_A$ 140.6 (1.50) *I* | *I* 136.2 (−1.56) $S_A$ 106.0 (−2.07) $S_{X2}$ 89.4 *g* |
| 100/0 | *K* 58.0 (2.26) $S_{X2}$ 117.3 (2.20) $S_A$ 141.7 (1.53) *I*<br>*g* 98.3 $S_{X2}$ 116.9 (2.24) $S_A$ 141.6 (1.54) *I* | *I* 136.0 (−1.56) $S_A$ 106.8 (−2.13) $S_{X2}$ 95.9 *g* |

[a]Data on the first line are from first heating and cooling scans. Data on the second line are from second heating scan. Heating and cooling rates are 10°C/min.

TABLE 7. Characterization of the Binary Mixtures of Poly(**15**) (DP = 14.8, $M_w/M_n$ = 1.12) with Poly(**16**) (DP = 14.5, $M_w/M_n$ = 1.13) (Polymer mixture III)

| Poly(**15**)/ poly(**16**), (mol)/(mol) | Phase transitions (°C) and corresponding enthalpy changes (kcal/mru)[a] | |
|---|---|---|
| | Heating | Cooling |
| 0/100 | *K* 55.1 (1.38) $S_{X2}$ 116.9 (2.32) $S_A$ 138.0 (1.21) *I*<br>*g* 83.9 $S_{X2}$ 116.6 (2.29) $S_A$ 137.6 (1.23) *I* | *I* 133.4 (−1.25) $S_A$ 107.0 (−2.27) $S_{X2}$ 75.2 *g* |
| 9.4/90.6 | *K* 64.2 (0.50) $S_{X2}$ 117.3 (2.13) $S_A$ 138.8 (1.14) *I*<br>*g* 80.4 $S_{X2}$ 116.9 (2.10) $S_A$ 138.6 (1.15) *I* | *I* 134.7 (−1.27) $S_A$ 108.3 (−2.11) $S_{X2}$ 73.3 *g* |
| 20.6/79.4 | *K* 70.3 (0.69) $S_{X2}$ 117.1 (2.27) $S_A$ 140.2 (1.21) *I*<br>*g* 78.4 $S_{X2}$ 117.6 (2.07) $S_A$ 140.8 (1.13) *I* | *I* 136.3 (−1.28) $S_A$ 109.3 (−2.12) $S_{X2}$ 74.2 *g* |
| 39.4/60.6 | *K* 62.4 (1.17) $S_{X2}$ 120.1 (2.21) $S_A$ 143.3 (1.21) *I*<br>*g* 80.7 $S_{X2}$ 120.0 (2.12) $S_A$ 144.1 (1.26) *I* | *I* 139.4 (−1.41) $S_A$ 111.7 (−2.14) $S_{X2}$ 72.9 *g* |
| 50.1/49.9 | *K* 65.4 (1.65) $S_{X2}$ 121.9 (2.26) $S_A$ 145.1 (1.26) *I*<br>*g* 85.9 $S_{X2}$ 122.5 (2.11) $S_A$ 146.3 (1.27) *I* | *I* 140.9 (−1.47) $S_A$ 113.1 (−2.19) $S_{X2}$ 74.7 *g* |
| 60.2/39.8 | *K* 63.3 (1.63) $S_{X2}$ 123.7 (2.18) $S_A$ 147.1 (1.28) *I*<br>*g* 80.7 $S_{X2}$ 124.0 (2.17) $S_A$ 147.7 (1.33) *I* | *I* 142.9 (−1.38) $S_A$ 114.4 (−2.15) $S_{X2}$ 74.8 *g* |
| 79.7/20.3 | *K* 65.9 (1.44) $S_{X2}$ 127.0 (2.18) $S_A$ 150.5 (1.38) *I*<br>$S_{X2}$ 126.5 (2.08) $S_A$ 151.5 (1.32) *I* | *I* 146.3 (−1.42) $S_A$ 116.4 (−2.03) $S_{X2}$ 106.5 *g* |
| 89.3/10.7 | *K* 69.1 (1.54) $S_{X2}$ 128.0 (2.21) $S_A$ 152.6 (1.33) *I*<br>*g* 107.1 $S_{X2}$ 127.6 (2.27) $S_A$ 152.2 (1.31) *I* | *I* 147.7 (−1.33) $S_A$ 117.3 (−2.18) $S_{X2}$ 100.0 *g* |
| 100/0 | *K* 59.4 (1.81) $S_{X2}$ 128.7 (2.42) $S_A$ 153.3 (1.36) *I*<br>*g* 110.6 $S_{X2}$ 128.4 (2.46) $S_A$ 153.1 (1.35) *I* | *I* 149.1 (−1.41) $S_A$ 118.3 (−2.41) $S_{X2}$ 104.2 *g* |

[a]Data on the first line are from first heating and cooling scans. Data on the second line are from second heating scan. Heating and cooling rates are 10°C/min.

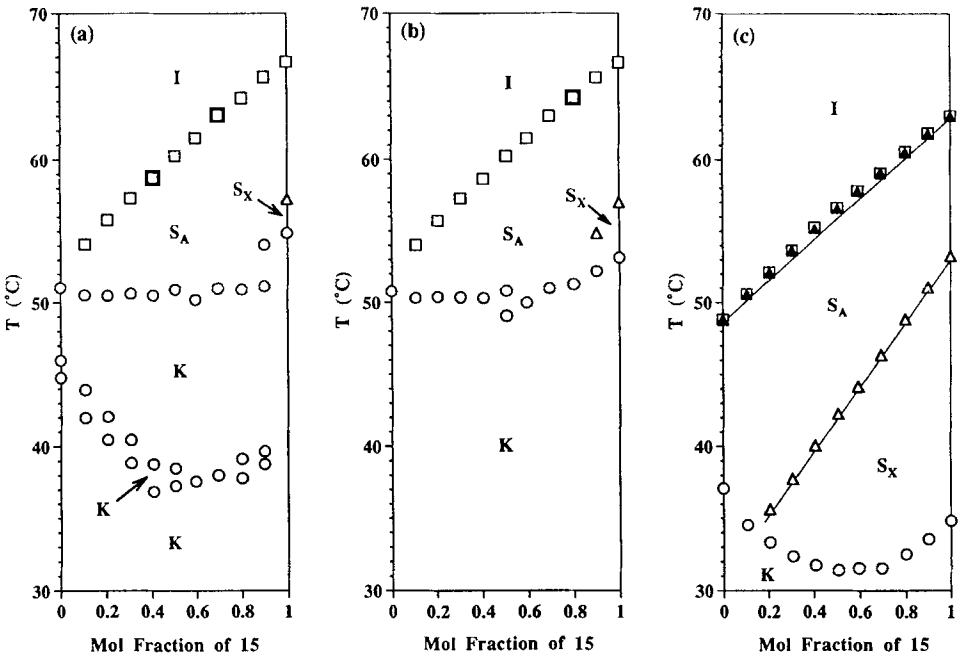


FIG. 9. Dependence of phase transition temperatures on the composition of the binary mixtures of **15** with **16**: (a) data from the first heating scans; (b) data from the second heating scans; (c) data from the first cooling scans. Open symbols represent experimental values; closed symbols represent ideal values calculated by the Schröder-van Laar equation.

from the linear dependence. Since the enthalpy change associated with the $S_A$-$I$ transition of monomer **15** is larger than that of monomer **16** (on the cooling scan, $\Delta H = -1.52$ cal/mol for the monomer **15** and $\Delta H = -1.24$ cal/mol for monomer **16**, see Table 4), the Schröder-van Laar equation [19, 20] gives a positive deviation from the linear dependence which corresponds to an ideal behavior. This is in good agreement with the experimental values in Fig. 9. This result suggests that there is no chiral molecular recognition in the $S_A$ phase of the monomer mixtures. It seems that the $S_X$-$S_A$ transitions of the first cooling scans follow a linear dependence on the composition except for the following two points: X/Y (**15**/**16**) = 0/100 and X/Y (**15**/**16**) = 10/90, whose data are not available because monomer **16** does not show the $S_X$ phase. The crystallization ($S_A$-$K$ or $S_X$-$K$) temperatures exhibit a low suppression ($-4.6$°C) with an eutectic point.

It can be seen from Figs. 10–12 that the three smectic phases ($S_A$, $S_{X1}$, and $S_{X2}$) show a continuous dependence on composition and, therefore, the two diastereomeric structural units derived from the two monomers are miscible and isomorphic in each smectic mesophase of the three sets of polymer mixtures. The $S_A$-$I$ transition temperatures are giving almost a linear dependence on the mixture composition for all polymer mixtures, and all experimental data (open symbols) are in good agreement with the calculated values (closed symbols) predicted by the Schröder-van Laar equation in Figs. 10–12, indicating the absence of chiral molecular recognition in the $S_A$ phase of the polymer mixtures. On the other hand, the $S_{X2}$-$S_A$ transition

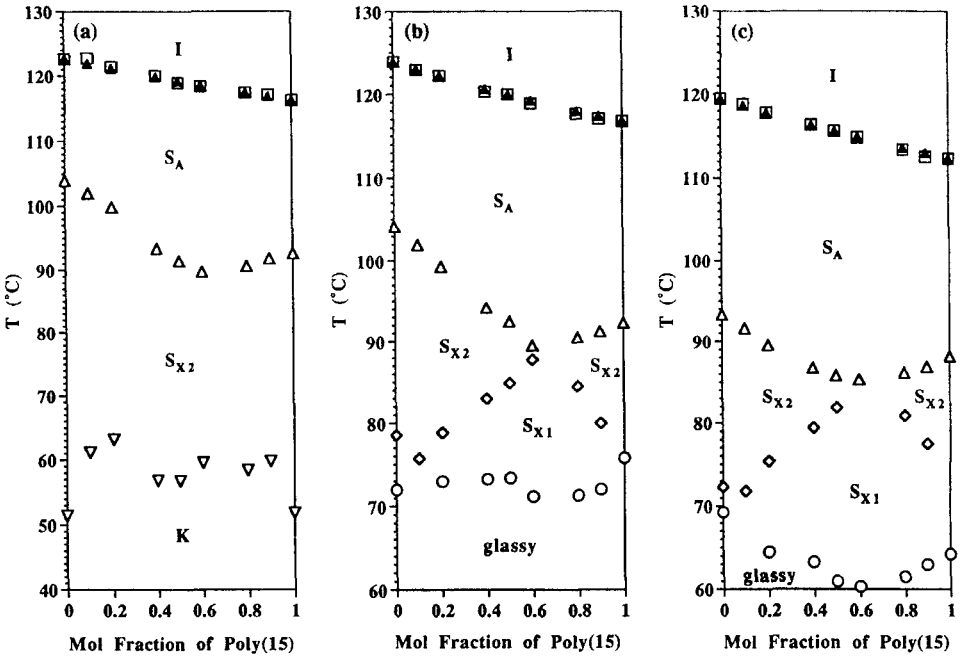


FIG. 10. The dependence of phase transition temperatures on composition of polymer mixture I [poly(**15**) (DP = 4.7) and poly(**16**) (DP = 9.0)]: (a) data from the first heating scans; (b) data from the second heating scans; (c) data from the first cooling scans. Open symbols represent experimental values; closed symbols represent ideal values calculated by the Schröder-van Laar equation.

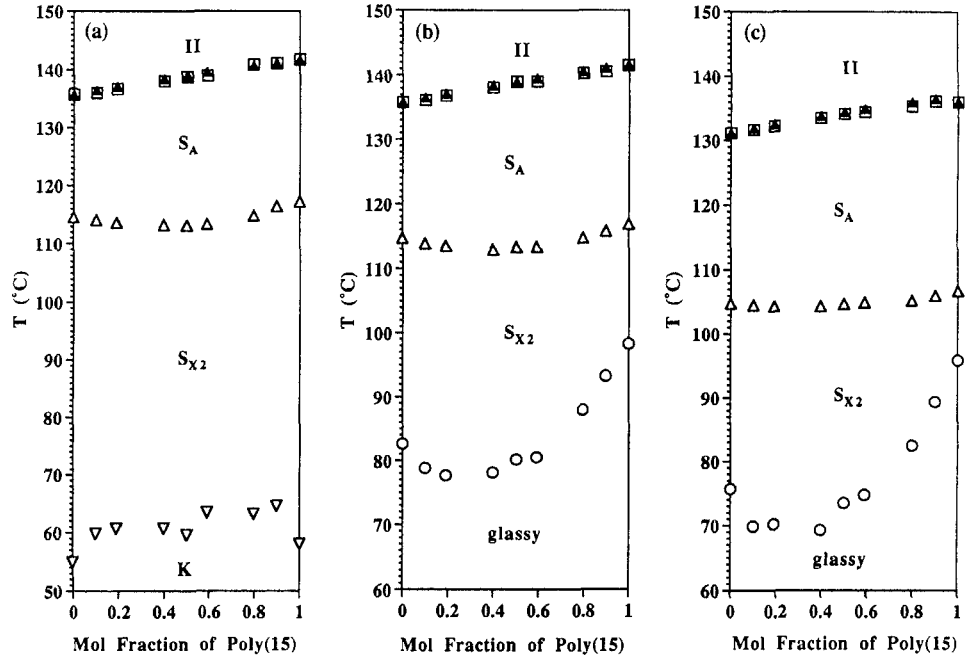


FIG. 11. The dependence of phase transition temperatures on composition of polymer mixture II [poly(**15**) (DP = 8.5) and poly(**16**) (DP = 12.5)]: (a) data from the first heating scans; (b) data from the second heating scans; (c) data from the first cooling scans. Open symbols represent experimental values; closed symbols represent ideal values calculated by the Schröder-van Laar equation.

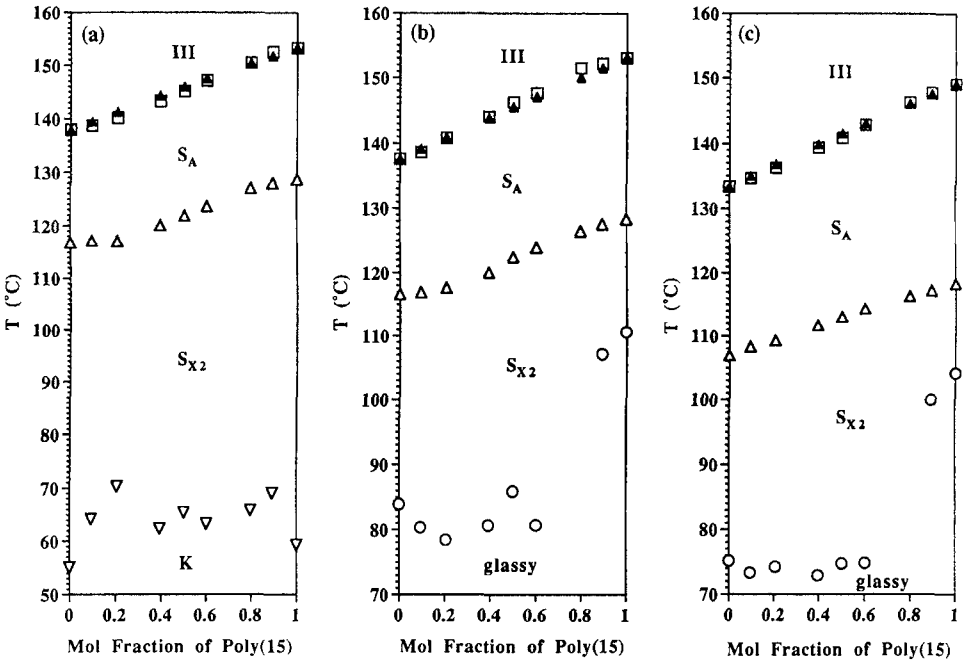


FIG. 12. The dependence of phase transition temperatures on composition of polymer mixture III [poly(**15**) (DP = 14.8) and poly(**16**) (DP = 14.5)]: (a) data from the first heating scans; (b) data from the second heating scans; (c) data from the first cooling scans. Open symbols represent experimental values; closed symbols represent ideal values calculated by the Schröder–van Laar equation.



temperatures are suppressed to show a downward curvature by mixing the two diastereomeric polymers. Polymer mixture I having the lowest molecular weights exhibits the largest deviation of the $S_{X2}$–$S_A$ transition temperatures from the ideal behavior, and this deviation is decreased with increasing the molecular weight of the polymers consisting the polymer mixtures (i.e., of polymer mixtures II and III). Polymer mixture I displays another transition between $S_{X1}$ and $S_{X2}$ mesophases. Judging from the DSC traces shown in Fig. 14, it seems that this transition is highly enhanced by mixing poly(**15**) and poly(**16**), suggesting that there is large chiral molecular recognition in the $S_{X1}$ phase between the two diastereomeric structural units of poly(**15**) and poly(**16**).

## SUMMARIES AND CONCLUSIONS

In the first paper of this series, we investigated and compared the phase behavior of two diastereomeric liquid crystalline monomers and polymers based on (2*R*,3*S*)- and (2*S*,3*S*)-2-fluoro-3-methylpentyl 4′-(11-vinyloxyundecanyloxy)biphenyl-4-carboxylate (**17**) [1]. The phase behaviors of (**2*R*,3*S*)-17** and (**2,*S*,3*S*)-17**, and corresponding polymers poly[(**2*R*,3*S*)-17**] and poly[(**2*S*,3*S*)-17**] were almost identical to each other. This result was unexpected and, therefore, of great interest

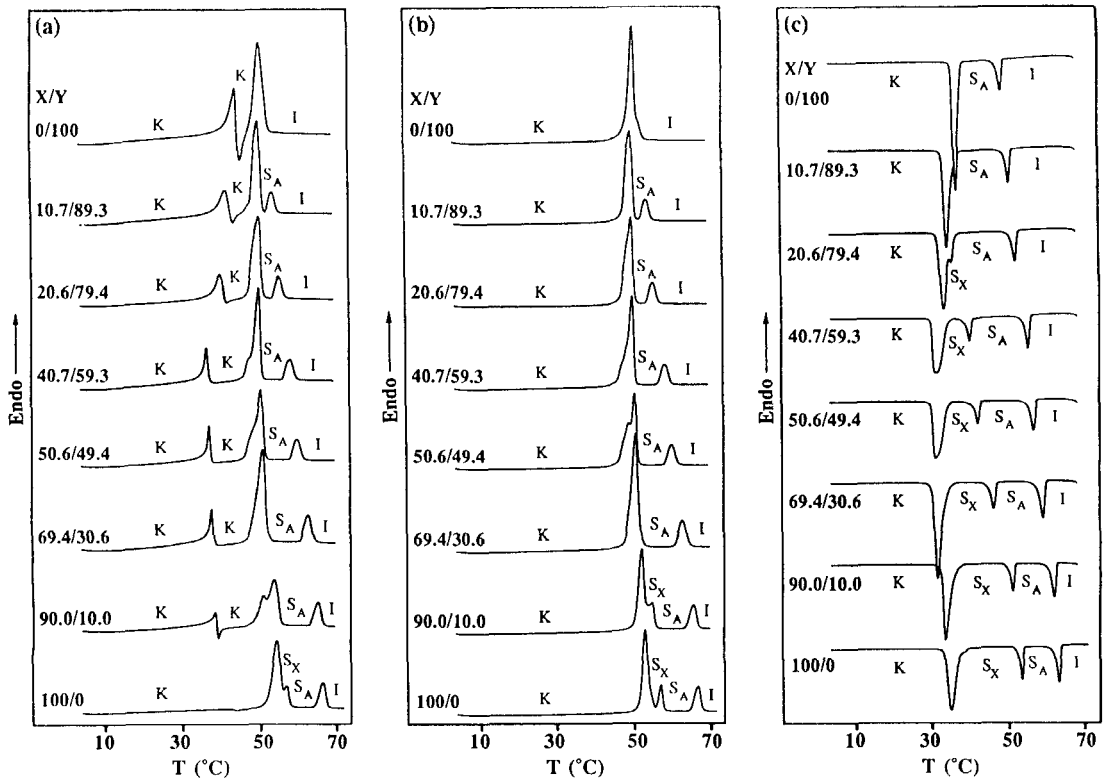


FIG. 13. DSC thermograms (10°C/min) of the binary mixtures of monomer **15** (X) with monomer **16** (Y): (a) first heating scans; (b) second heating scans; (c) first cooling scans.

since two diastereomers usually exhibit different physical properties. The monomers **15** and **16** used in the current study have a similar structure to **17**, and the only structural difference lies in the direction of the ester function which connects the biphenyl mesogen and the chiral tail. However, the phase behaviors exhibited by **15** and **16**, and poly(**15**) and poly(**16**) are totally different from those of **17** and poly(**17**) in the following two points: 1) **15** and **16**, and poly(**15**) and poly(**16**) do not show a $S_C^*$ phase, which was observed in both diastereomers of **17** and poly(**17**); 2) **15** and **16**, and poly(**15**) and poly(**16**) display identical mesophases. However, their transition temperatures are different, i.e., **15** and poly(**15**) show *ca.* 15–20°C higher transition temperatures than **16** and poly(**16**).

With respect to the chiral molecular recognition, the $S_A$–*I* transition of the binary mixture of (**2*R*,3*S*)-17** with (**2*S*,3*S*)-17** was within 0.2–0.4°C higher in the 50/50 mixture than the theoretical value expected for an ideal solution, and it was suggested that chiral molecular recognition was present in the $S_A$ phase between the two diastereomers. In the polymer systems, on the contrary, the chiral recognition observed in monomers seemed to be canceled or too small to be detected. In the current study, monomers **15** and **16**, and polymers poly(**15**) and poly(**16**) also showed the $S_A$ phase; however, chiral molecular recognition was not detected in any

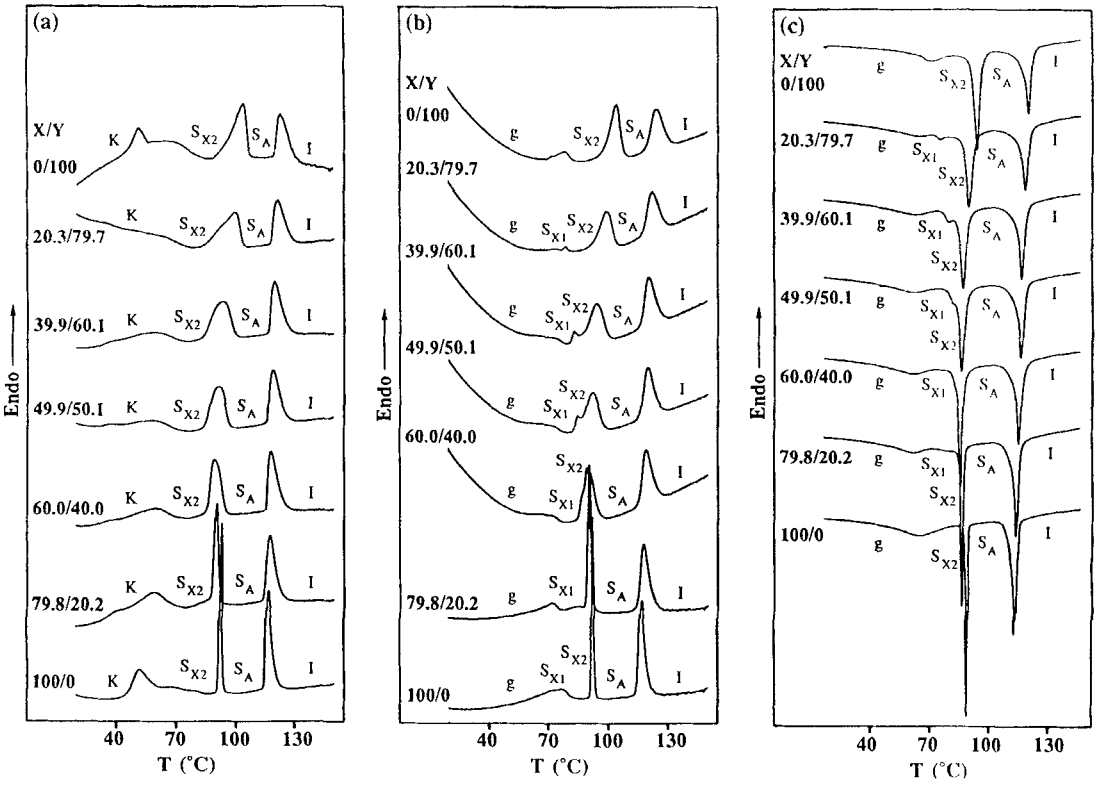


FIG. 14. DSC thermograms (10°C/min) of polymer mixture I [poly(**15**) (DP = 4.7) (X) and poly(**16**) (DP = 9.0) (Y)]: (a) first heating scans; (b) second heating scans; (c) first cooling scans.

of the monomer or polymer mixtures. The reason for the disappearance of the chiral molecular recognition in the $S_A$ phase by the reversal of the ester function is not clear. The reversal of the ester function results in the disappearance of the methylene group which connects the ester group and the chiral center. We first expected that this disappearance of the methylene group would cause the restricted rotation of the chiral tail due to the steric hindrance and, as a consequence, enhance the chiral molecular recognition. At the same time, however, the dipole moments of the carbonyl group and the C—F bond point out the opposite direction, resulting in the decrease of the total dipole moment of the molecule. It is possible to speculate that this decrease of the total dipole moment reduces the molecular intraction and, subsequently, makes the chiral molecular recognition too small to be detected.

## ACKNOWLEDGMENT

Financial support by the Office of the Naval Research is gratefully acknowledged.

## REFERENCES


[1] V. Percec, H. Oda, P. L. Rinaldi, and D. R. Hensley, *Macromolecules, 27*, 12 (1994).

[2] V. Percec and H. Oda, *Ibid., 27*, 4454 (1994).

[3] V. Percec and H. Oda, *Ibid., 27*, 5821 (1994).

[4] (a) J. Jacques, A. Collet, and S. H. Wilen, *Enantiomers, Racemates and Resolutions*: Krieger Publishing Co., Malabar, 1991; (b) M. Leclercq, J. Billard, and J. Jacques, *Mol. Cryst. Liq. Cryst., 8*, 367 (1969); (c) C. H. Bahr, G. Heppke, and B. Sabaschus, *Ferroelectrics, 84*, 103 (1988); (d) C. H. Bahr, G. Heppke, and B. Sabaschus, *Liq. Cryst., 9*, 31 (1991).

[5] (a) Y. Yamada, K. Mori, N. Yamamoto, H. Hayashi, K. Nakamura, M. Yamawaki, H. Orihara, and Y. Ishibashi, *Jpn. J. Appl. Phys., 28*, L1606 (1989); (b) H. Takezoe, J. Lee, A. D. L. Chandani, E. Gorecka, Y. Ouchi, A. Fukuda, K. Terashima, and K. Furukawa, *Ferroelectrics, 114*, 187 (1991); (c) H. Takezoe, A. Fukuda, A. Ikeda, Y. Takanishi, T. Umemoto, J. Watanabe, H. Iwane, M. Hara, and K. Itoh, *Ibid., 122*, 167 (1991); (d) J. W. Goodby and E. Chin, *Liq. Cryst., 3*, 1245 (1988); (e) J. W. Goodby, J. S. Patel, and E. Chin, *J. Mater. Chem., 2*, 197 (1992); (f) G. Heppke, D. Lötzsch, D. Demus, S. Diele, K. Jahn, and H. Zaschke, *Mol. Cryst. Liq. Cryst., 208*, 9 (1991).

[6] (a) J. W. Goodby, M. A. Waugh, S. M. Stein, E. Chin, R. Pindak, and J. S. Patel, *J. Am. Chem. Soc., 111*, 8119 (1989); (b) A. J. Slaney and J. W. Goodby, *Liq. Cryst., 9*, 849 (1991); (c) J. W. Goodby, I. Nishiyama, A. J. Slaney, C. J. Booth, and K. J. Toyne, *Ibid., 14*, 37 (1993); (d) H. T. Nguyen, R. J. Twieg, M. F. Nabor, N. Isaert, and C. Destrade, *Ferroelectrics, 121*, 187 (1991); (e) L. Navailles, H. T. Nguyen, P. Barois, C. Destrade, and N. Isaert, *Liq. Cryst., 15*, 479 (1993).

[7] (a) A. M. Levelut, C. Germain, P. Keller, L. Liebert, and J. Billard, *J. Phys., Paris, 44*, 623 (1983); (b) P. Keller, *Mol. Cryst. Liq. Cryst. Lett., 102*, 295 (1984); (c) J. Billard, A. Dahlgren, K. Flatischler, S. T. Lagerwall, and B. J. Otterholm, *J. Phys., Paris, 46*, 1241 (1985); (d) G. Heppke, P. Kleineberg, and D. Lötzsch, *Liq. Cryst., 14*, 67 (1993).

[8] For a brief review on the molecular engineering of side chain LCP by living cationic polymerization see: V. Percec and D. Tomazos, *Adv. Mater, 4*, 548 (1992); (b) V. Percec and D. Tomazos, "Molecular Engineering of Liquid Crystalline Polymers," in *Comprehensive Polymer Science, First Suppl.* (G. Allen, Ed.), Pergamon Press, Oxford, 1992, pp. 299–383; (c) V. Percec and D. Tomazos, in *Contemporary Topics in Polymer Science, Vol. 7, Advances in New Materials* (J. C. Salamone and J. Riffle, Eds.), Plenum Press, New York, 1992; (d) V. Percec and D. Tomazos, "Recent Developments in Tailor-Made Liquid Crystalline Polymers," in *Frontiers in Macromolecular Chemistry*, Special Issue of *Indian J. Technol., 31*, 339–392 (1993).

[9] (a) V. Percec, Q. Zheng, and M. Lee, *J. Mater. Chem., 1*, 611 (1991); (b) V. Percec, Q. Zheng, and M. Lee, *Ibid., 1*, 1015 (1991); (c) V. Percec and Q. Zheng, *Ibid., 2*, 475 (1992); (d) V. Percec and Q. Zheng, *Ibid., 2*, 1041 (1992).

[10] (a) T. Sierra, E. Meléndez, J. L. Serrano, A. Ezcurra, and M. A. Pérez-Jubindo, *Chem. Mater., 3*, 157 (1991); (b) T. Sierra, J. L. Serrano, M. B. Ros, A. Ezcurra, and J. Zubia, *J. Am. Chem. Soc., 114*, 7645 (1992); (c) T. Sierra, M. B. Ros, A. Omenat, and J. L. Serrano, *Chem. Mater., 5*, 938 (1993).

[11] (a) K. Yoshino, S. Kishio, M. Ozaki, T. Sakurai, N. Mikami, R. Higuchi, and M. Honma, *Jpn. J. Appl. Phys., 25*, L416 (1986); (b) K. Yoshino, M. Ozaki, S. Kishio, T. Sakurai, N. Mikami, R. Higuchi, and M. Honma, *Mol. Cryst. Liq. Cryst., 144*, 87 (1987); (c) M. Ozaki, K. Yoshino, T. Sakurai, N. Mikami, and R. Higuchi, *J. Chem. Phys., 86*, 3648 (1987).

[12] (a) R. J. Twieg, K. Betterton, H. T. Nguyen, W. Tang, and W. Hinsberg, *Ferroelectrics, 91*, 243 (1991); (b) B. Shivkumar, B. K. Sadashiva, S. Krishna Prasad, and S. M. Khened, *Ibid., 114*, 273 (1991).

[13] J. E. McKeon and P. Fitton, *Tetrahedron, 28*, 233 (1972).

[14] (a) V. Percec, M. Lee, and H. Jonsson, *J. Polym. Sci., Polym. Chem. Ed., 29*, 327 (1991); (b) V. Percec and V. Lee, *Macromolecules, 24*, 1017 (1991); (c) V. Percec, M. Lee, P. Rinaldi, and V. E. Litman, *J. Polym. Sci., Polym. Chem. Ed., 30*, 1213 (1992).

[15] (a) C. G. Cho, B. A. Feit, and O. W. Webster, *Macromolecules, 23*, 1918 (1900); (b) C. G. Cho, B. A. Feit, and O. W. Webster, *Ibid., 25*, 2081 (1992); (c) C. H. Lin and K. Matyjaszewski, *Polym. Prepr., Am. Chem. Soc., Div. Polym. Chem., 31*, 599 (1990).

[16] (a) V. Percec and M. Lee, *Polymer, 32*, 2862 (1991); (b) V. Percec and M. Lee, *Polym. Bull., 25*, 131 (1991); (c) V. Percec and M. Lee, *Macromolecules, 24*, 4963 (1991); (d) V. Percec and M. Lee, *J. Mater. Chem., 1*, 1007 (1991); (e) V. Percec and M. Lee, *Ibid., 2*, 617 (1992).

[17] (a) J. W. Goodby and T. M. Leslie, *Mol. Cryst. Liq. Cryst., 110*, 175 (1984); (b) C. R. Walton and J. W. Goodby, *Mol. Cryst. Liq. Cryst. Lett., 92*, 263 (1984); (c) J. W. Goodby, and T. M. Leslie, in *Liquid Crystals and Ordered Fluids*, Vol. 4 (A. C. Griffin and J. F. Johnson, Eds.), Plenum Press, New York, 1984, p. 1; (d) J. W. Goodby (Ed.), *Ferroelectric Liquid Crystals. Principles, Properties and Applications*, Gordon and Breach Science Publishers, Philadelphia, 1991.

[18] (a) M. Tabrizian, C. Bunel, J.-P. Vairon, C. Friedrich, and C. Noël, *Makromol. Chem., 194*, 689 (1993); (b) M. Tabrizian, C. Bunel, J.-P. Vairon, C. Friedrich, and C. Noël, *Ibid., 194*, 891 (1993).

[19] (a) G. R. Van Hecke, *J. Phys. Chem., 83*, 2344 (1979); (b) M. F. Achard, M. Mauzac, H. Richard, G. Sigaud, and F. Hardouin, *Eur. Polym. J., 25*, 593 (1989).

[20] (a) V. Percec and M. Lee, *J. Mater. Chem., 1*, 1007 (1991); (b) V. Percec, M. Lee, and Q. Zheng, *Liq. Cryst., 12*, 715 (1992); (c) V. Percec and G. Johansson, *J. Mater. Chem., 3*, 83 (1993).